Cell Reports
Physical Science

CellPress
OPEN ACCESS

Review

Wearable sensors and devices for real-time cardiovascular disease monitoring

Jian Lin,[1,3,5] Rumin Fu,[2,3,5] Xinxiang Zhong,[1,3] Peng Yu,[2,3] Guoxin Tan,[4] Wei Li,[2,3] Huan Zhang,[2,3] Yangfan Li,[2,3,*] Lei Zhou,[2,3,*] and Chengyun Ning[1,2,3,*]

SUMMARY

Cardiovascular disease (CVD) is a major global health problem. Living with diseases like CVD often requires long-term monitoring, for which flexible and conformable sensors are employed. The developments in materials, devices, integrated electronic systems, the Internet of Things (IoT), and edge computing enable real-time and convenient measurement and detection of signals. Herein, we review the latest developments in the surveillance of various physiological signals of flexible sensors for CVD. First, a variety of signals that can monitor CVD are summarized. Then, the different mechanisms and principles of monitoring pulse signals, as well as the flexible sensor monitoring of electrocardiogram (ECG), phonocardiogram (PCG), seismocardiogram/ballistocardiogram (SCG/BCG), and apexcardiogram (ACG) signals are discussed. Finally, future research directions are proposed based on the current research landscape.

INTRODUCTION

In recent years, although living standards have gradually improved, living habits and diet have become more and more irregular, which is known to increase the burden on the heart and likely to cause heart disease. "Report on Cardiovascular Health and Diseases in China 2019: An Updated Summary"[1] pointed out that the prevalence of cardiovascular diseases (CVDs) in China has been rising year after year, and it is estimated that there are 330 million cardiovascular patients, and the mortality rate of CVD ranks first among all diseases. Not only that, but the cost of CVD treatment is also very expensive. The World Heart Federation has estimated that by 2030, the total global cost of CVD treatment will increase from approximately USD 863 billion in 2010 to a staggering USD 1,044 billion.[2] As a result, the prevention of CVD plays a vital role in reducing the mortality and cost of CVD treatment.

The cardiovascular condition can be obtained from some signals generated during the rhythmic heartbeat. Electrocardiogram (ECG) signals are produced since the heart has a special electrical signal conduction system. This conduction system is composed of differentiated cardiomyocytes. Cardiomyocytes are excited by the sinoatrial node, and then the electrical signal spreads to the atria and ventricles in a certain path and time sequence, and finally synthesizes the ECG signal on the body surface. The opening and closing of each valve during a heartbeat produces a heart sound signal. Along with the cyclical contraction of the heart, the pulse waves generated by the arteries combine various information carried by the heart pumping activity and pressure waves along the arterial tree. A complex and weak force is generated in the process of pumping blood, and seismocardiogram/ballistocardiogram (SCG/BCG) signals are generated based on

[1]School of Biomedical Sciences and Engineering, South China University of Technology, Guangzhou 510006, China

[2]School of Materials Science and Engineering, South China University of Technology, Guangzhou 510641, China

[3]National Engineering Research Center for Tissue Restoration and Reconstruction, South China University of Technology, Guangzhou 510006, China

[4]School of Chemical Engineering and Light Industry, Guangdong University of Technology, Guangzhou 510006, China

[5]These authors contributed equally

*Correspondence: liyf87@scut.edu.cn (Y.L.), zhoul@scut.edu.cn (L.Z.), imcyning@scut.edu.cn (C.N.)

https://doi.org/10.1016/j.xcrp.2021.100541

the force and reaction force. At the same time, the apex hits the chest wall during the heartbeat and generates an apexcardiogram (ACG) signal. These signals can partly reflect cardiovascular conditions. Nowadays, some commercial monitoring equipment, whether it is a blood pressure meter, an ECG device (Holter), or a mattress system that monitors BCG/SCG signals, are relatively bulky and inconvenient to carry, and the electrodes can easily fall off.[3] These traditional monitoring methods will have a bad influence on people's normal work and study.

A new flexible electronic technology is expected to solve these problems. Flexible electronics are lightweight, sensitive, etc., which can adapt to human skin very well.[4–9] Recently, the development of flexible materials and processing technology has made it possible to monitor the situation of human body for a long time through flexible wearable sensors and devices.[10,11] Especially with the popularization of the 5th Generation Mobile Communication Technology (5G) plus edge computing and the Internet of Things (IoT), it will help flexible electronics to reach a higher level in monitoring. In the future, the health management of people will be more personalized and precise with these new information technologies.

In some previous review articles, Hong et al.[10] discussed flexible electronic devices such as ECG, blood pressure, blood oxygen, and implantable therapy. Feng's team[12] reviewed the research progress of flexible electronics in bioelectrical signals, biophysical signals, and biochemical signals from the aspects of material, structure, and device design. Chen et al.[13] focused on the progress in materials, structures, and mechanisms of flexible sensors used for heart rate, blood pressure, blood oxygen, and blood glucose monitoring. These reviews have very good guiding significance for researchers in their respective research fields.

In this review, we present recent research on flexible sensing technologies and devices used for the prevention of CVD. First, we describe the five human signals for monitoring CVD and briefly review the characteristics and generation principles of these signals.[12,14] In addition, we introduce several pulse wave parameters that reflect cardiovascular conditions. Then, around these five signals, the flexible sensing technology and equipment developed in recent years are reviewed from the perspective of materials and manufacturing processes. Different sensing mechanisms are classified, and the flexible sensing technology of pulse wave signals is introduced in detail. Finally, we briefly summarize and look forward to the future of monitoring cardiovascular conditions by flexible sensing technology and equipment.

CVD AND SIGNALS

CVDs have an important impact on human health, especially for the elderly, and most CVDs are chronic. Moreover, the treatment period is long, thus posing a great threat to the health of patients. The use of non-invasive devices for prediagnosis and therapeutic monitoring of cardiovascular parameters not only enables the early diagnosis of CVD but also helps to improve the quality of life of patients. This has a positive impact on the doctor's ability to treat patients according to their cardiovascular condition and plays an important role in protecting patients' lives and reducing the incidence of CVD.[15]

Non-invasive cardiovascular parameters are mainly measured by measuring pulse wave, ECG, PCG, PPG, and SCG/BCG. However, in related studies, pulse wave, and heart sound alone has been studied more. In particular, flexible sensing has focused on pulse waves. The various signal waveforms are shown in Figure 1.

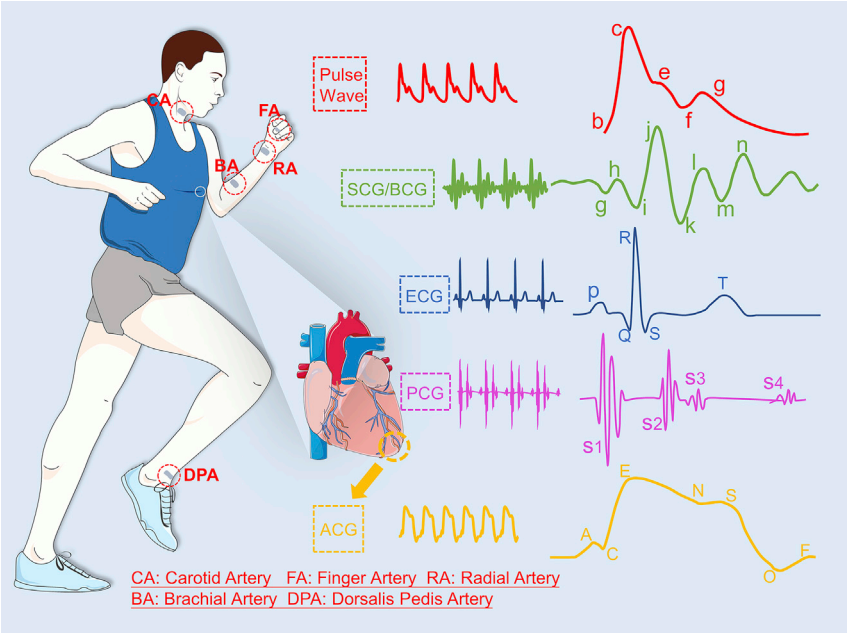

Figure 1. Schematic illustration of multiple physiological signals for the prevention of CVD
Physiological signals include pulse wave, SCG/BCG, ECG, PCG, and ACG.

Pulse wave signal

Pulse wave analysis (PWA) is an emerging technique for the assessment of arterial elasticity and has become an important technique for the early detection of arteriosclerosis.[16,17] The PWA method extracts and calculates the cardiovascular function indexes based on the time-domain characteristics of the pulse waveform and the corresponding pathophysiological information, which is incomparably superior to the traditional imaging methods. Pulse wave detection methods are categorized according to the location of detection, and the commonly used ones are CA (carotid artery), DA (digital artery), RA (radial artery), BA (brachial artery), and DPA (dorsalis pedis artery)[18] (Figure 1). The typical time amplitude curve of a pulse waveform is shown in red in Figure 1. For example, a standard RA waveform contains the following five features: (1) point b: the trough of the pulse wave, i.e., the beginning of the wave, which marks the beginning of the rapid ejection period and is the lowest point in the whole pulse wave; (2) point c: the first systolic waveform of the pulse wave, called the main waveform peak. At point c, the evacuation volume of the left ventricle is comparable to that of the aorta, which reflects the maximum value of arterial pressure and pulse volume; (3) point e: the second systolic peak of the pulse wave, also known as the reflection point; it usually appears after the main wave and its position is below the main wave; (4) point f: the descending isthmus, also known as the trough of the dicrotic pulse; it is mainly a downward tangential wave composed of the descending and ascending branches of the beat wave; the trough of the bicep wave is the boundary point of cardiac contraction and diastole; (5) point g: the peak of the dicrotic pulse, which corresponds to the diastolic peak of the cardiac cycle; it is formed when the aortic arch accommodates blood during systole and releases it during diastole and hits the aortic valve rebound. Among the above characteristic points, the reflected wave produced by them is relatively weak, so the identification of point e is the most difficult,[18–20] but its clinical application value is significant. Therefore, the study of the e-point recognition algorithm has been a research hot spot in the field of PWA.[21]

Table 1. Principles and classification of different cardiovascular parameters

Parameter	Category	Principle	Explanation
PWV	PVP	$PWV = \frac{L}{PTT}$	L, the length between two recording body parts
SV	CFP	$SV = \frac{0.283}{K^2} T(P_s - P_d)$	K, relative position of the mean pulse wave; T, period
CO	CFP	$CO = SV\frac{60}{T} = \frac{17}{K^2}(P_s - P_d)$	—
CI	CFP	$CI = CO/BSA$	BSA, body surface area
SEVR	CFP	$SEVR = \frac{DPTI}{SPTI}$	DPTI, diastolic-pressure time index; SPTI, systolic-pressure time index
TPR	PVP	$TPR = \frac{P_m}{CO}$	—
PI	PVP	$PI = \frac{AC\ component}{DC\ component}$	AC, alternative current; DC, direct current
AI	PVP	$AI = \frac{SBP2-DBP}{SBP1-DBP}$	SBP1, first peak systolic blood pressure; SBP2, second peak systolic blood pressure; DBP, diastolic blood pressure
C1	PVP	$C_1 = 2A_4\frac{(A_2+A_4)^2+A_5}{RA_2(2A_4+A_2)(A_4^2+A_5^2)}$	A2, A4, attenuation constant; A5, oscillation frequency; R, total peripheral resistance
C2	PVP	$C_2 = \frac{1}{R(2A_4+A_2)}$	—
ABI	PVP	$ABI = \frac{Pa}{Pu}$	Pa, ankle systolic pressure; Pu, systolic pressure on the upper arm

Studies have shown that many cardiovascular parameters can be obtained from pulse waves, and there are many products available in the market for the assessment of cardiovascular status through pulse waves. In terms of classification, cardiovascular parameters can be generally classified into two categories: cardiac function parameters (CFPs) and peripheral vascular parameters (PVPs). This corresponds to two kinds of testing techniques: CFP testing techniques and PVP testing techniques. Non-invasive CFP tests include doppler echocardiography, impedance differential cardiograms, various stress tests, ECGs, phonocardiograms, apical and carotid pulse diagrams, and pulse diagrams. Ultrasound doppler and cardiac impedance mapping are the more commonly used methods. The invasive tests mainly include the FICK method and the thermodilution method. PVPs are measured by continuous ultrasound doppler, by pulse transducer, and most commonly by various monitors. In general, CFPs are mainly cardiac index (CI), cardiac output (CO), and stroke volume (SV). PVPs mainly include systolic Ps, diastolic Pd, pulse pressure Pn (Ps-Pd), mean arterial pressure Pm, heart rate (HR), pulse wave velocity (PWV), and many other indicators, such as subendocardial viability ratio (SEVR), total peripheral resistance (TPR), perfusion index (PI), augmentation index (AI), capacitive compliance (C1), oscillatory compliance (C2), and ankle-brachial index (ABI).[22,23] See Table 1 for these indicators and principles.

Heart sound signal

From the perspective of prevention, in the early stages of the onset of certain CVDs, changes in heart sound signal can often indicate the arrival of certain diseases, so heart sound signal has an irreplaceable role in early diagnosis of CVD. The PCG is shown in pink in Figure 1. The first heart sound S1 is produced by atrioventricular valve closure, marking the onset of ventricular contraction. The second heart sound S2 is produced by the closure of the arterial valve, marking the onset of ventricular diastole. The third heart sound S3 occurs in the early stage of ventricular diastole. The fourth heart sound S4 occurs in the late stage of ventricular diastole. It has been shown that changes in first heart sound amplitude are positively correlated with the rate of increase in left ventricular pressure,[24] and that changes in left ventricular pressure have an independent effect on first heart sound intensity, which is a standard measure of myocardial contractile energy.[25] Therefore, the study of the

energy distribution of the heart sound signal and the total energy magnitude is a preliminary assessment of the state of the cardiac energy reserve.

The frequency and intensity of the heart sound signal are indicative of myocardial function and the condition of heart valves and intracardiac blood flow. In the study of the relationship between heart sound signal characteristics and heart disease, the analysis method is mainly to use modern digital signal processing tools to analyze the heart sound signal in the time domain and frequency domain and to use machine learning or deep learning to classify and diagnose heart sound signals and diseases.

ECG signal

ECG is one of the most common methods for the diagnosis of CVD, providing objective indicators in the proper analysis, diagnosis, treatment, and monitoring of heart disease. It has been widely used in clinical practice. One of the most important parameters reflecting cardiovascular health is the heart rate obtained by ECG. By monitoring the heart rate, some information about the rate and rhythm of the heartbeat can be obtained, which is important for CVD monitoring cardiopulmonary function assessment. The normal ECG is shown in the blue waveform in Figure 1, and the general ECG signal is composed of P waves, QRS clusters, and T waves.

The analysis of ECG signals is divided into two aspects: time domain and frequency domain. In addition to some commonly used waveform intervals and amplitude parameters in the time domain, heart rate variability (HRV) can also reflect cardiovascular conditions.[26] HRV is defined as the variation in beat-by-beat cycle differences, which indicates the extent to which the cardiovascular system is under sympathetic and parasympathetic control reflecting information about the modulation of the cardiovascular system by neurohumoral factors. HRV is a predictor of myocardial infarction mortality and can be used as a basis for the determination of CVD. HRV also plays an important role in the prevention and treatment of hypertension, myocardial infarction, sudden cardiac death, and arrhythmia. The detection and analysis of HRV are of great significance to the prevention and diagnosis of CVD.

It is also similar to the study of heart sound signals, which mainly involves the use of machine learning and deep learning to classify heart signals and achieve a diagnosis of disease. This is particularly important for signal acquisition. In the future, the popularity of flexible wearable electrodes will produce even greater amounts of data. By making good use of big data and artificial intelligence, people can understand their cardiovascular status in real-time, daily, which will effectively reduce the mortality of CVD.

SCG/BCG signal

Although ECG is commonly used in clinical applications to examine cardiac function, this method requires direct contact between the electrodes and the human skin and is not suitable for prolonged application in cardiac function testing. SCG/BCG is a faint mechanical signal produced by the heart's pumping activity that causes the body to vibrate synchronously and contains a large amount of important information related to the cyclic activity of the heart. The SCG/BCG signal also enables non-contact, non-sensory detection of cardiac function with the human body, making it ideal for long-term cardiac function monitoring.

Detection devices based on the SCG/BCG signal allow the insensitive monitoring of the heart's mechanical activity without the need to attach the sensor directly to the body.[27,28] The SCG/BCG and its cycle are useful for studying the physiology of the

cardiac cycle. As shown in the green waveform in Figure 1, the ideal SCG/BCG waveform consists of eight parts, which are the waveform information indicated by g, h, i, j, k, l, m, and n. Under normal conditions, the BCG signal should be consistent with the human heartbeat and show a distinct periodicity. Among the g, h, i, j, k, l, m, and n segments of the BCG signal, the h, i, j, k, and l bands have the greatest amplitude. Experts in cardiac signaling usually call the h, i, j, k, and l combination the W[29] combination wave, based on its shape.

It is generally accepted that h, i, j, and k waves are associated with cardiac contraction; m and n waves are associated with cardiac diastole. The amplitude of i-j during inspiration is greater than the amplitude during expiration, but its deviation is always within a moderate range. In the SCG of each cardiac cycle, the waveform produced during systole is predominant. The waveform produced during diastole is smaller in amplitude. The pattern is coherent and repeatable. There are normal respiratory variations in amplitude, and the amplitude is within a certain empirical range. Due to differences in the structure of the body and the instruments used, the details recorded will vary, but the overall shape is essentially similar.

ACG signal

ACG signal is an electrical signal recorded by the pressure transducer, which is a change in the surface pressure of the chest wall caused by the apex of the heart hitting the chest wall. In fact, ACG reflects the relationship between pressure and volume of the changing left ventricle. It can accurately reflect the changes in the relative vibration of each period of the cardiac cycle, which is of practical value.[30] ACG has become a commonly used non-invasive technique for testing cardiac function. The ACG waveform is shown in orange in Figure 1, with A wave being the atrial systolic wave; C is the starting point of ventricular systole, followed by the SW wave (ventricular systolic wave); E is the apex of the SW wave, the apex of ejection; P is the turning point of the descending branch of SW and the transition from rapid to slow ejection; S is the slow ejection wave; O is the lowest point of the descending branch of SW and marks the opening of the mitral valve; F is the junction point of RFW (fast filling wave) and SFW (slow filling wave), which is also called the fast filling stop point.

FLEXIBLE SENSORS FOR CVD MONITORING

Since flexible stretchable silicon was reviewed as one of the top 10 technologies by the MIT Technology Review in 2006,[31] research on flexible sensors made of flexible materials[32–37] for human health monitoring is getting deeper and deeper. Most of the research used for non-invasive monitoring of CVD focuses on a series of signals generated during the beating of the heart, such as pulse waves, heart sounds, ECG, SCG/BCG, and ACG signals. Their similarities and differences are shown in Table 2.

Pulse waves

Numerous studies have shown that the pulse signal reflects the cardiovascular status of the human body. Pulse wave detection can be divided into applanation tonometry and (gas or optical) plethysmography according to the principle.[18] In addition to these two types, there are two other types that are measured by accelerometer and impedance plethysmography, but these two methods are not commonly used.[38,39] The applanation tonometry method involves fixing the pressure transducer to the superficial artery and using signal conversion to record the pulse wave. Plethysmography is commonly used for cuff inflation measurements, where the cuff of the sphygmomanometer is attached to the brachial and/or ankle arteries to record the pulse wave. Photoplethysmography (PPG) is used to acquire and analyze pulse wave signals from the digital arteries. This section focuses on the

Table 2. Principles and classification of different cardiovascular parameters

Signal	Detection part	Signal source	Signal type	Sensor requirements	Advantage/ disadvantage
Pulse Wave	mainly on wrist	arteries	mechanical signal	sensitive, thin, breathable	simple but difficult to accurately monitor
ECG	twelve-lead	sinus node	electric signal	low impedance, stable, breathable	accurate, but contact with skin
PCG	aortic valve and pulmonary valve area	heart valve	mechanical signal	low noise, thin	fast, non-invasive but weak, high noise
PPG	mainly on finger	arteries	photoelectric signal	accurate, breathable	low cost, non-invasive, easy to operate
ACG	—	apex	mechanical signal	non-toxic	simple but weak,
SCG/BCG	—	—	mechanical signal	high sensitivity	non-contact but weak

different sensing mechanisms in pressure sensing and introduces the latest developments in flexible sensors based on piezoresistance, capacitive pressure sensor, self-powered (including piezoelectric and based on friction nanogenerators), and PPG.

Piezoresistive sensors are favored by researchers because of their low fabrication cost, high sensitivity, and the simple process of fabricating their sensitive elements. Some one-dimensional and two-dimensional conductive materials and conductive polymers such as silver nanowires (AgNWs),[40–43] graphene,[42,44–53] Mxene,[40,54–62] carbon nanotubes (CNTs),[63–66] and polyaniline (PANI)[67] have been applied to sensors for monitoring human pulse wave signals. The performance of the sensor is enhanced by building different sensing microstructures together with some substrate materials such as hydrogels[4,55,64,67] and polydimethylsiloxane (PDMS).[41,44,46,63]

Ji et al.[41] constructed a solid microdome array dual conductive layer sensor using cyclohexane polydimethylsiloxane (CPDMS)/AgNWs as shown in Figure 2A. This sensor offers both sensitivity and linearity, with a linear range of 0–70 kPa and a sensitivity of 924.37 kPa^{-1}, making it a versatile wearable platform. From the perspective of bionics, Choi's team[68] was inspired by the phenomenon of spiders using crack-like organs near the joints of their legs to sense very small changes in mechanical stress, and fabricated nanoscale crack sensors. Similarly, Liu et al.[69] were also inspired by the cilia and cracks of spiders and used Co and Pt to fabricate ultra-sensitive multifunctional sensors (Figure 2B). In order to reuse the sensor after damage, Liao et al.[64] combined functionalized SCNT (FSCNT) and hydrogel to obtain a self-healing and adherent epidermal sensor for pulse monitoring (Figure 2C). The healing ability of the sensor is 99% after 2 s, and it has an adhesive nature due to the presence of polydopamine (PDA). In another study, Wu et al.[53] fabricated a triode-mimicking positive graphene pressure sensor (TMPGPS) by laser engraving reduced graphene oxide (Figure 2D). This sensor is capable of reproducing the blood pressure waveform of the human body from the pulse wave signal. In addition to the carbon-based materials above, Guo et al.[58] used the two-dimensional material MXene to make a degradable sensor for monitoring the human radial artery and made an array to monitor pressure (Figure 2E). Generally speaking, piezoresistive sensors can be designed with different structures using different materials to obtain a function similar to skin sensing. Piezoresistive sensors of different structures and materials are shown in Table 3. In the future, wearable piezoresistive sensors will continue to improve the sensitivity, accuracy, and detection range and will develop toward multifunctional sensing.

One of the biggest reasons why self-powered sensors are of interest to researchers is that they are self-powered and do not require an external power supply, which can

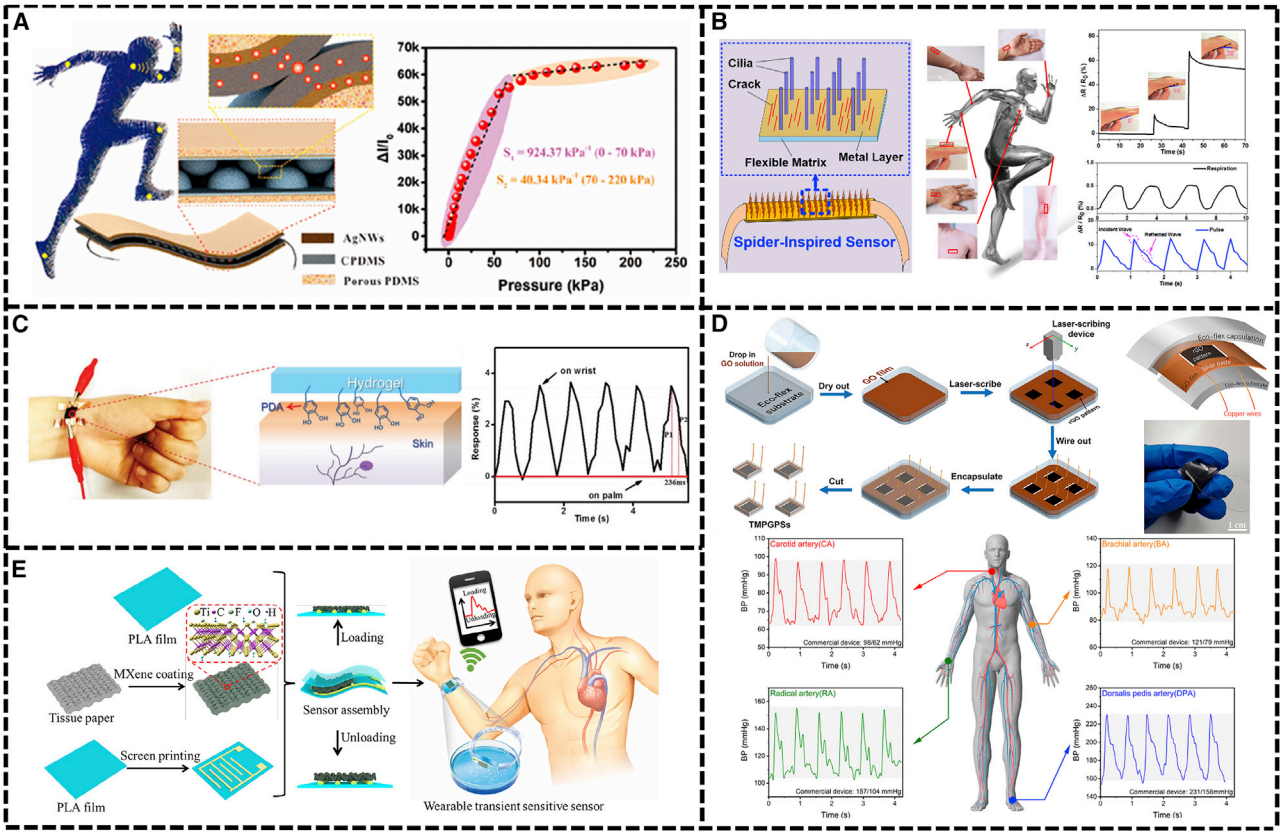

Figure 2. Flexible piezoresistive sensors are used for pulse wave monitoring

(A) Sensor assembly with interlocked microdome arrays (left); relative current variation of the CPDMS/AgNW DCL-based sensor with interlocked porous dome structure (right). Adapted with permission from Ji et al.[41]. Copyright 2020, American Chemical Society.

(B) Schematic showing the piezoresistive cilia and cracks model inspired by the spider (left) that monitors human body motion and health-related signals: finger bending, respiration, and wrist blood pulse (right). Adapted with permission from Liu et al.[69] Copyright 2020, American Chemical Society.

(C) Self-adhered on the wrist during the human-machine interaction and healthcare monitoring (left); the tiny movement caused by pulse (right). Copyright 2017, Wiley. Used with permission from Liao et al.[64]

(D) Sensor and schematic process of the low-cost and easy fabrication of TMPGPS (top); blood pressure waveforms, and values collected at carotid artery (CA), brachial artery (BA), radial artery (RA), and dorsalis pedis artery (DPA) (bottom). Adapted with permission from Wu et al.[53] Copyright 2020, American Chemical Society.

(E) Schematic illustration of the fabrication procedure of flexible wearable transient pressure sensors with MXene nanosheets. Adapted with permission from Guo et al.[58] Copyright 2019, American Chemical Society.

reduce energy consumption in the system.[77] The self-powered mechanisms are mainly based on the piezoelectric effect or friction-electric nanogenerators.[78] In order to apply this to the detection of human pulse waves, researchers have done a lot of work to continuously improve its sensitivity and minimum detection limit to achieve the detection of small changes in human pulse. As shown in Figure 3A, Fu et al.[79] reported a piezoelectric hydrogel to enhance the β-phase content of PVDF by dipole interaction between PAN and PVDF. This piezoelectric hydrogel can be used to monitor the human body radial artery. Similarly, Chu et al.[80] used (fluorinated ethylene propylene) (FEP) and Ecoflex materials to fabricate a sandwich structure piezoelectret (Figure 3B). This sensor can imitate the pulse in traditional Chinese medicine (TCM) and measure the pulse wave signals of three different parts—cun, guan, and chi—on human arms at the same time. The RR interval is obtained from the pulse wave, and then the poincare plots can be plotted using the RR interval to distinguish people with arrhythmias from those without arrhythmias. In addition

Table 3. Flexible piezoresistive sensors are used for pulse wave detection

Ref.	Electrode	Active materials	Structure	Sensitivity	Analysis	Technology
[41]	—	CPDMS/AgNWs	SDA	>40.34 kPa^{-1}	no	dip/spin-coating
[46]	IDE	PDMS/graphene	micropatterns	1,875.53kPa^{-1}	yes	self-assembled
[43]	Ag paste	AgNWs/rGO	hierarchical	134 kPa^{-1}	no	Electrospinning
[52]	Cr/Au	PTNWs/graphene	band	9.4 × 10^{-3} kPa^{-1}	no	drop-casting
[68]	Cr/Pt	Cr/Pt	patterned crack	1 × 105 kPa^{-1}	no	thermal evaporation
[69]	Al	Co/Pt	cilia/crack	0.5 mV/g	no	magnetron sputtering
[58]	IDE	MXene/tissue	sandwiching porous	2.52 kPa^{-1}	no	screen printing
[64]	Cu	PVA/FSWCNT/PDA	—	—	no	—
[44]	Ag paste	rGO	RDS	25.1 kPa^{-1}	no	template
[60]	Ag paste	MXene	texture	>178.4	no	—
[54]	Ag	MXene/serine	—	107.43	yes	latex assembly
[62]	IDE	MXene/PVB	—	>0.2 kPa^{-1}	no	—
[55]	—	MXene/ hydrogel	—	—	no	—
[65]	Ag paste	SWNT	protrusive	1.80 kPa^{-1}	no	spin-coated
[48]	Au	rGO/PVDF	interlocked microdome	35 μA/Pa	yes	rod casting
[70]	Pt	rGO	porous	282.28	no	spin-coated
[50]	—	LSG	multilayer	673	no	CVD
[53]	Ag paste	LSG	sandwich	4–7 kPa^{-1}	yes	laser engraving
[45]	Ag	graphene	crisscross	>500	yes	CVD
[51]	silver paint	GOLCs/KGM	porous	0.28 kPa^{-1}	no	self-assembly
[49]	Cu	CGF	—	101 kPa^{-1}	yes	electrospinning
[57]	IDE	MXene/PVANWs	3D network	>147 kPa^{-1}	no	dipping-drying
[71]	stainless steel	WK	molecular spring	0.30 kPa^{-1}	yes	—
[72]	Cu	P-TDI-IP/Au	interlock	3.32 kPa^{-1}	no	laser
[73]	Ag paste	PANI/PAA/PA	porous structure	37.6 kPa^{-1}	yes	—
[59]	IDE	MXene	microspinous	151.4 kPa^{-1}	no	magnetron sputtering
[61]	Au/Cr	MXene/NMC	interlocked	24.63 kPa^{-1}	yes	vacuum evaporation
[40]	—	MXene/AgNWs/ PDA/ Ni^{2+}	brick-and-mortar	>200	no	screen-printing
[42]	—	GO/AgNWs/C60	lamellar	2,392.9	no	screen-printing
[74]	Ag paste	AgNP/PEDOT/paper	—	0.119 kPa^{-1}	no	—
[56]	Cu	MXene/hydrogel	3D network	80	no	—
[47]	—	PDCY/rGO	double-sided arch	—	yes	—
[67]	Cu	PANI/P(AAm-co-HEMA)	—	11	no	—
[75]	ITO	ZnO	urchin-shaped	121 kPa^{-1}	no	solution process
[76]	Cu	CB	—	51.23 kPa^{-1}	no	drop-casting

CPDMS, cyclohexane polydimethylsiloxane; NWs, nanowires; SDA, solid microdome array; IDE, interdigital electrode; rGO, reduced graphene oxide; PTNWs, $PbTiO_3$ nanowires; PVA, polyvinyl alcohol; SWCNT, single wall carbon nanotube; FSWCNT, functionalized SWCNT; PDA, polydopamine; PVB, polyvinyl butyral; PVDF, poly(vinylidene fluoride); PAN, polyacrylonitrile; LSG, laser scribed graphene; CVD, chemical vapor deposition; GO, graphene oxide; GOLCs, graphene oxide liquid crystals; KGM, konjac glucomannan; CGF, carbonized gelatin film; WK, wool keratin; P-TDI-IP, polytetramethylene glycol (P), 2,40-tolylene diisocyanate (TDI), and isophorone diisocyanate (IP); PANI, polyaniline; PAA, polyaniline; PA, phytic acid; NMC, natural microcapsule; PEDOT, poly(3,4-ethylenedioxythiophene); PDCY, polyurethane double covered yarn; P(AAm-co-HEMA), poly(acrylamide-co-hydroxyethyl methyl acrylate); CB, carbon black.

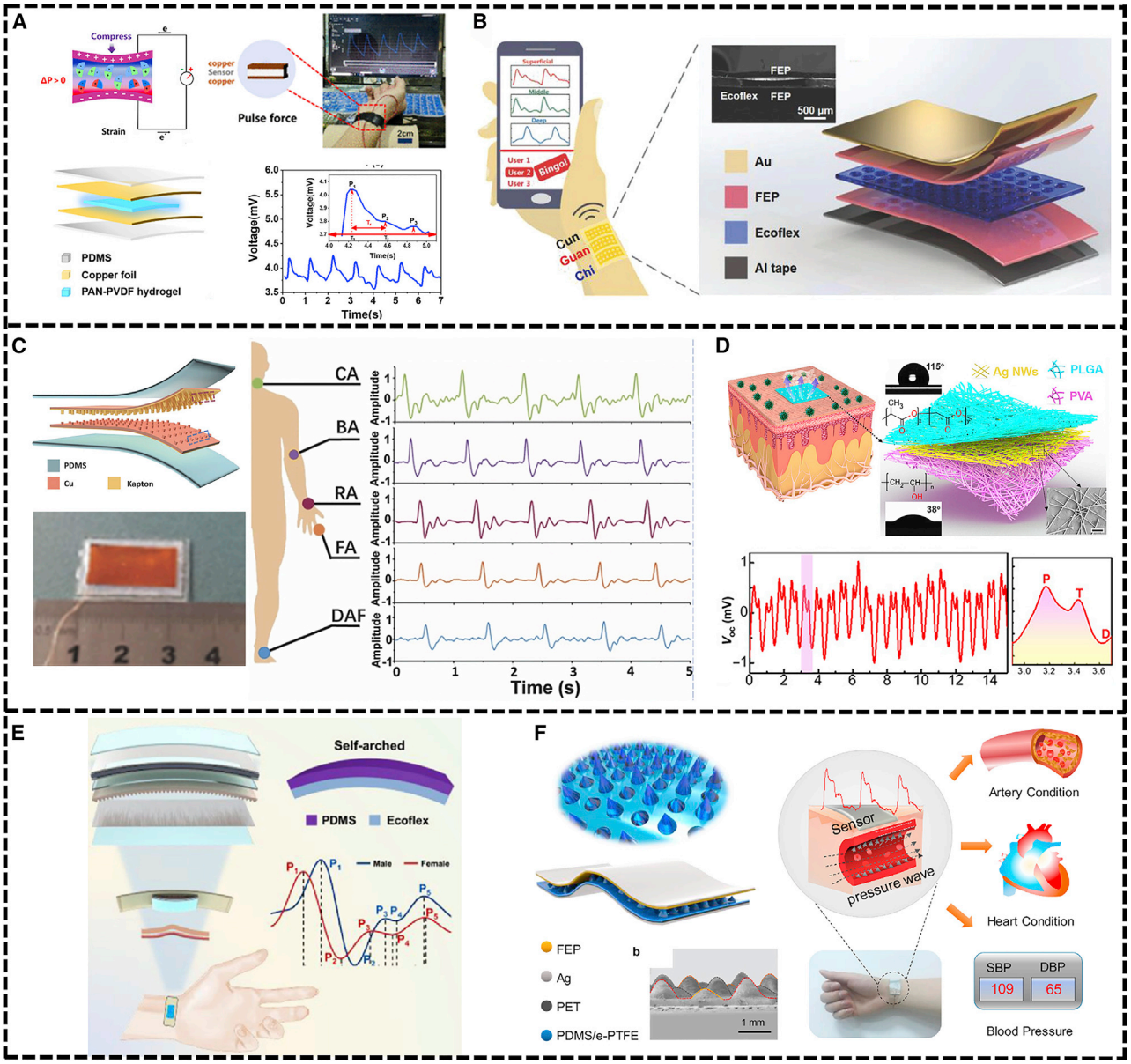

Figure 3. Flexible self-powered pressure sensors are used for pulse wave monitoring

(A) PAN/PVDF hydrogel sensor for measuring the radial artery. Reproduced with permission.[79] Copyright 2019, American Chemical Society.

(B) Piezoelectric sensing system for pulse wave detection. Copyright 2018, Wiley. Used with permission from Chu et al.[80]

(C) Schematic diagram of TENG and photograph of the size (2 cm × 1 cm) of SUPS (left); the signal output of SUPS pressed on various artery position(right). Copyright 2017, Wiley. Used with permission from Ouyang et al.[88]

(D) Structural design of the all-nanofiber TENG-based e-skin (top) and real-time monitoring of the radial artery pulse (bottom). Reproduced with permission.[89] Copyright 2020, AAAS.

(E) Schematic diagram of the structure of SANG and comparison of single-cycle pulse waveform of male and female experimenters. Adapted from Zou et al.[90] with permission from Elsevier.

(F) Schematic structure of HSPS and the capability of multifunctional cardiovascular motoring. Adapted from Chen et al.[83] with permission from Elsevier.

to the aforementioned PVDF[36,81,82] and FEP,[80,83] some other active materials, like group III N compounds,[84] PZT,[85–87] etc., have also been used as sensitive elements.

The research on friction electrode-based sensors has flourished since 2012 when Wang's team[91] proposed friction nanogenerators. As shown in Figure 3C, Wang's

team[88] used inductively coupled plasma (ICP) to etch Kapton and copper film to obtain a self-powered ultra-sensitive pulse sensor (SUPS) with a nano-scale concave structure. The use of this sensor can accurately, wirelessly, and continuously monitor pulse signals in the cardiovascular system in real-time. At the same time, the characteristic exponent analysis of the pulse signals of patients with coronary heart disease, atrial septal defect, and atrial fibrillation can provide indicative diagnosis and antidiastolic treatment for CVD. Then they made a breathable, biodegradable, and antibacterial friction nanogenerator electronic skin.[89] This sensor was made by sandwiching AgNWs between polylactic acid (PLGA) and polyvinyl alcohol (PVA) and applied for whole-body physiological signal monitoring such as human pulse monitoring (Figure 3D). For better stability and output, Zou et al.[90] fabricated a sensor with a unique self-arching structure by adjusting the mass ratio of two silicone elastomers, PDMS and Ecoflex. This sensor integrates frictional and piezoelectric effects together for the diagnosis of arterial stiffness (Figure 3E). For the same purpose, Chen et al.[83] reported an electrostatic nanogenerator-based self-powered pressure sensor based on hierarchical elastomer microstructures (HEM) (Figure 3F) in response to previous studies that could not simultaneously obtain high sensitivity and wide pressure range. This sensor has a sensitivity of up to 7.989 V kPa^{-1} in the range of 0.1–60 kPa and can be used for multifunctional monitoring of cardiac and vascular conditions. Although there have been many papers on self-powered pressure sensors to monitor the cardiovascular status of the human body,[92] it is still a big challenge to make a fully flexible monitoring system that does not rely on external power sources for power supply.[93] A summary of the materials and structures of the sensitive components developed by the self-powered flexible sensor for CVD monitoring reported in recent years is shown in Table 4.

Capacitor devices have relatively high-pressure strain sensitivity and are not sensitive to temperature. The change of capacitance can be used to detect the change of pressure. The capacitance can be directly energized to detect, or detected by the natural frequency of the circuit in the detector, which does not need a power supply. Bao's team[99] recently developed a degradable *in vivo* sensor based on fringe-field capacitor technology for continuous monitoring of arterial blood flow after microvascular reconstruction surgery. They chose poly(glycerol sebacate) (PGS), a material used in tissue engineering, as the sensitive element and selected a pyramid structure to increase its sensitivity. A radio frequency reader was used to read the frequency variation, and thus the blood flow information could be obtained, but this is an invasive method for implantation. Generally, for direct detection of capacitance changes, the relationship between deformation and capacitance, $C = \varepsilon S/4\pi kd$ (where C is the capacitance, ε is the dielectric constant of the dielectric layer, S is the effective area of the conductive layer, k is the electrostatic constant, and d is the thickness of the dielectric layer), is used.[4,100] Most of the flexible capacitive sensors are based on this formula. As shown in Figure 4A, Sudeep Sharma et al.[101] used PVDF-TrFE/MXene as the dielectric layer and the stress to simultaneously change the ε and d of the dielectric layer for sensing. In addition to PVDF-TrFE,[102] the materials used in the dielectric layer include PDMS,[103–105] polypropylene (PP),[106] polyurethane (PU),[107] and hydrogels,[108,109] etc. For example, Zhu et al.[109] employed Nafion as a sensitive element to fabricate a capacitive sensor with an epidermal electro-ionic interface (EII) (Figure 4B). This sensor used the epidermis to form a capacitive layer, which achieved high-pressure sensitivity and high signal-to-noise ratio, and it could monitor human blood pressure signals. To improve sensitivity, Zhao et al.[107] produced 3D AgNWs@TPU network composite films by electrospinning technology (Figure 4C). Similarly, Lin et al.[103] combined PDMS ion gel and PVDF-HFP to make a capacitive pressure sensor (Figure 4D). This sensor has a low-pressure

Table 4. Flexible self-powered pressure sensors are used for pulse wave detection

Ref.	Electrode	Active materials	Structure	Sensitivity	Analysis	Technology
[82]	Au	PVDF	laminated	114.2 mV/μm	no	electrospinning
[79]	Cu	PAN/PVDF	sandwich	—	yes	copolymerization
[84]	Ni/Au/ Cu/Au	III-N	sandwich	(0.24/0.2) mV/um	yes	layer-transfer
[81]	Al	PVDF/HHE	laminated	1,154 V/cm^3	yes	electrospinning
[94]	—	PZT	laminated	—	yes	—
[87]	Cu	PZT	—	—	yes	—
[86]	IDE	PZT	—	0.018 kPa^{-1}	yes	ILLO
[85]	Au	PZT	capacitor-type	0.005 Pa	yes	sol-gel
[80]	Al/Au	FEP	sandwich	32.6 nA kPa^{-1}	yes	spin-coated
[95]	Al	PAMPS	dihedral stripes	1.76 VN^{-1}	no	spin-coated
[88]	Cu	Kapton	concave	1.52 V	yes	ICP etching
[89]	Cu	PLGA/AgNWs/ PVA	sandwich	0.011 kPa^{-1}	no	electrospinning
[96]	Ag	PVDF	—	—	yes	serigraphy
[90]	Ag/Al	PVDF/Ecoflex	self-arched	—	yes	—
[83]	Ag	FEP/PDMS/ e-PTFE	hierarchical	7.989 VkPa^{-1}	yes	magnetron sputtering
[97]	Mg	SNRF/RSFF	—	—	no	—
[98]	Cu	PVA/gelatin	—	—	yes	—

HHE, hydroxylamine hydrochloride; IDE, interdigital electrode; ILLO, inorganic-based laser lift-off; PAMPS, poly(2-acrylamido-2-methyl-1-propanesulfonic acid); NWs, nanowires; e-PTFE, expanded fibrous poly tetra fluoroethylene; SNRF, silk nanoribbon film; RSFF, regenerative silk fibroin film.

range of 0.01 to 1.5 kPa. With a high sensitivity of 0.43 kPa^{-1}, it can detect human pulse (Figure 4E).

The pulse wave is divided into applanation tonometry and (gas or optical) plethysmography. The most common plethysmography is the photoelectric conversion method based on Lambert Beer's law.[110] The detection of superficial parts of the human body such as earlobes and fingertips is called photoplethysmography (PPG). Nowadays, the flexible PPG method mainly starts from two aspects. One is to make use of existing integrated chips on a flexible material substrate, and the other is to make flexible organic light-emitting materials and photosensitive materials into flexible light-emitting diodes and flexible photodetector, respectively. On the one hand, John's team[111,112] is committed to the design of flexible integrated systems. They used a serpentine trace and folded island structure to combine the integrated circuit chip ingeniously with a flexible substrate and used it instead of wired monitoring equipment in an intensive care unit (ICU) to monitor a baby's ECG and pulse wave (Figure 5A). This was conducive to better monitoring of infants. On the other hand, as shown in Figure 5B, Polat et al.[113] used graphene sensitized with semiconducting quantum dots as a photodetector, which was flexible, transparent, and had broadband wavelength sensitivity (300 to 2000 nm). In order to reduce power consumption, Lee et al.[114] obtained a relatively good detector layout (Figure 5D) from the study of light reflection in skin blood vessels (Figure 5C) so that its power consumption was only 10 mW (Figure 5E). For the same purpose, Xu et al.[115] mixed organic phototransistors (OPTs) (Figure 5F) and inorganic light-emitting diodes to reduce their low power and selected infrared light as the medium to detect pulse waves to improve the detection sensitivity. At the same time, the average systolic blood pressure (SBP) and average diastolic blood pressure (DBP) measured by the near-infrared hybrid PPG (hPPG) were compared to commercial reflective PPG (cPPGG), and commercial cuff-based devices (Figure 5F). Kim et al.[116] fabricated a stretchable light-emitting diode (LED) and a stretchable photoelectric sensor based

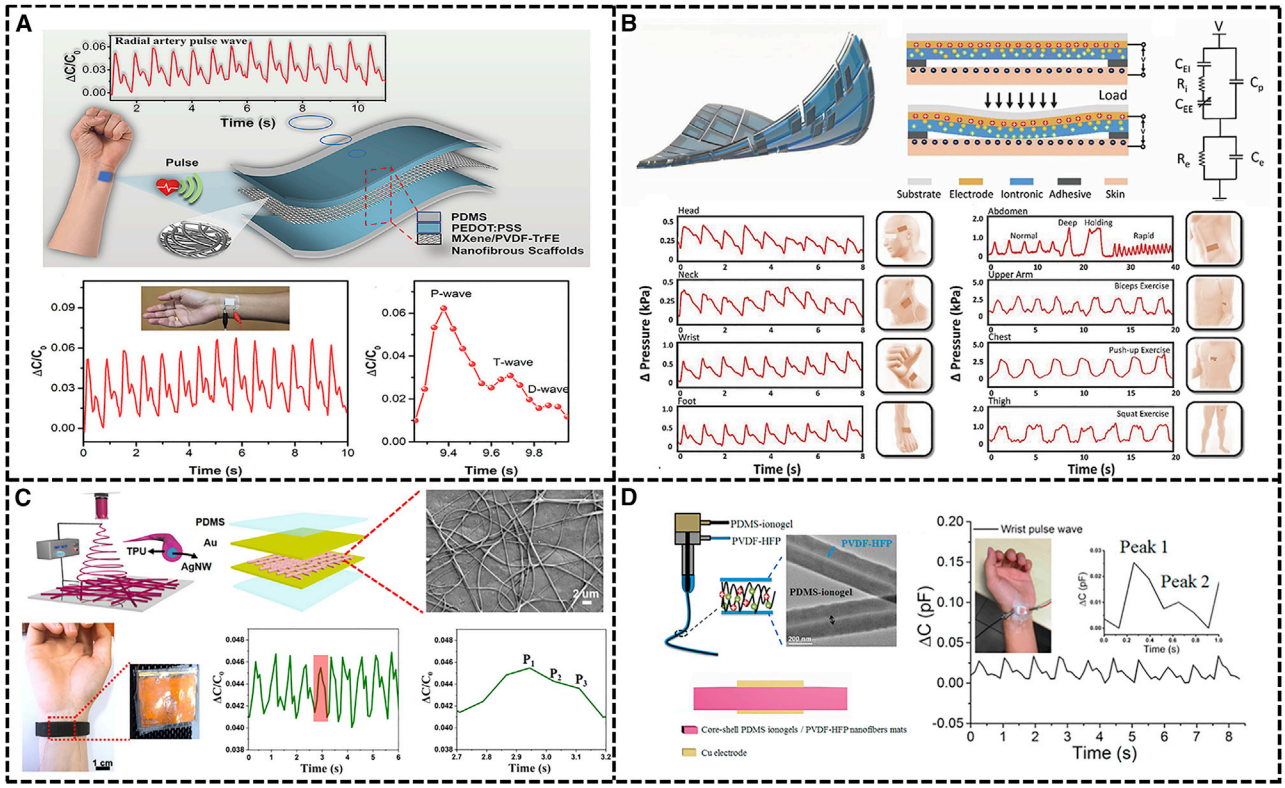

Figure 4. Flexible capacitive pressure sensors are used for pulse wave monitoring

(A) Illustration of the pressure sensor with structure of the composite nanofibrous scaffolds (top) and its real-time monitoring of the radial artery pulse wave (bottom). Adapted with permission of American Chemical Society.

(B) Perspective view of sensor (top left), cross-sectional view of the EII devices (top center), and the equivalent electrical circuit mode (top right); signals detected in different parts of the body (bottom). Copyright 2018, Wiley. Used with permission from Zhu et al.[109]

(C) Manufacturing process diagram of the 3D AgNWs@TPU NCFs and schematic illustration of the flexible capacitive sensor (top); measurement of the radial artery (bottom). Adapted with permission from Zhao et al.[107] Copyright 2020, American Chemical Society.

(D) Illustration of the process for preparing core-shell PDMS ion gel/PVDF-HFP nanofibers and its TEM image (top); device configuration of the pressure sensor (bottom); the real-time pressure waveforms of the measured heart rate. Adapted from Lin et al.[103] with permission from Elsevier.

on a combination of quantum dots, flexible substrates, and graphene for pulse wave detection, and all parts of this device were flexible (Figure 5G).

The time-domain signal of the pulse wave can more intuitively reflect the CVD status. The Young's modulus of the flexible sensor mentioned in the article can basically correspond to the human skin, and the research mainly focused on the sensitivity and linear range. However, the flexible sensor still has certain challenges in monitoring several characteristic points of the pulse wave, as well as the monitoring of blood pressure and other parameters through the pulse wave. In the future, with the in-depth research on pulse wave signals, the combination with flexible sensing technology will be more conducive to the prevention of CVD.

PCG

Cardiac auscultation is one of the commonly used medical diagnostic methods. It can provide valuable information about heart valve function and hemodynamics and yield many cardiac conditions such as arrhythmias, valve disease, and heart failure. Heart sound signals play an important role in the early detection of CVD. Recording the heart sound signal in time and amplitude is called a phonocardiogram. Nowadays, heart sound sensors are mainly produced from the direction of

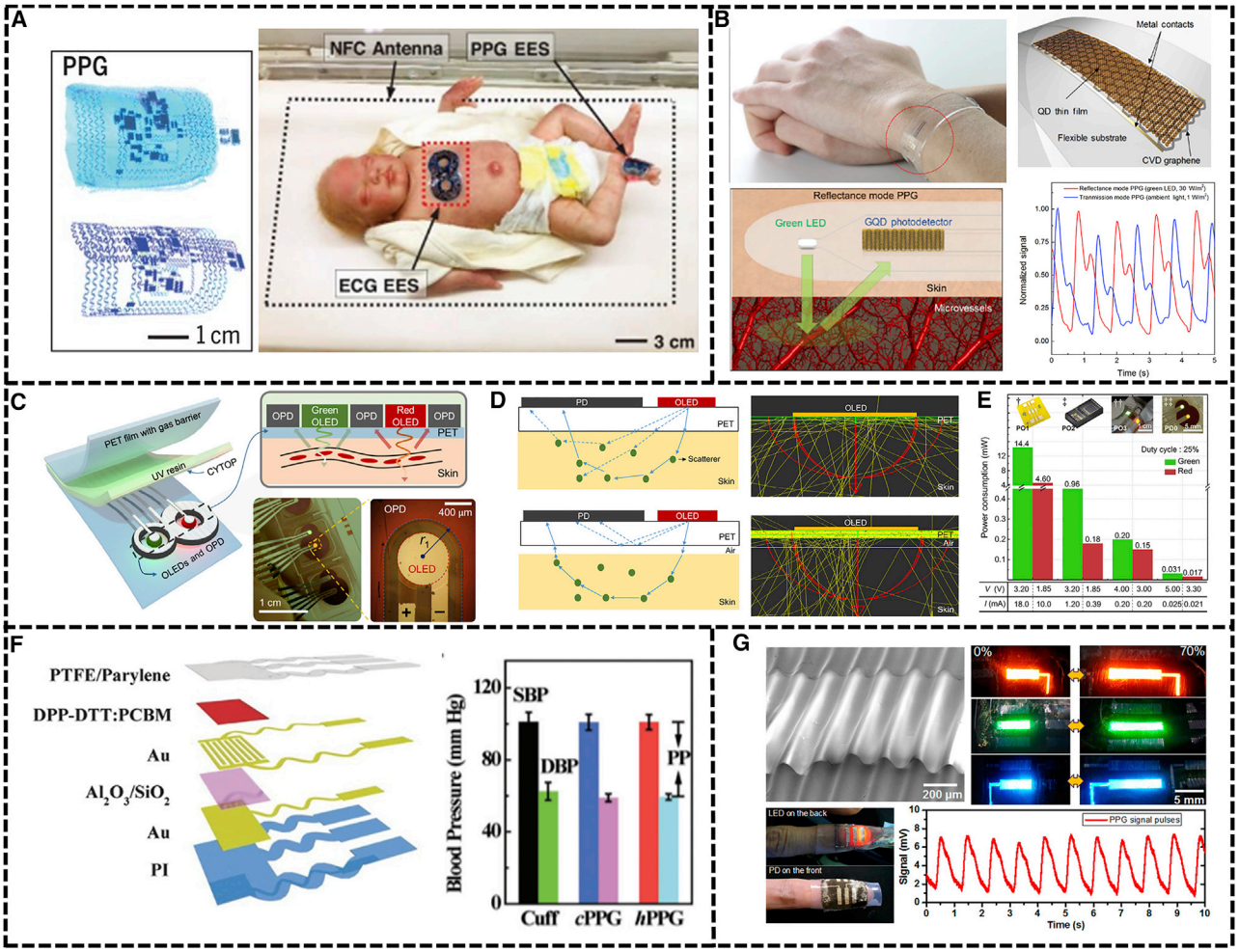

Figure 5. Flexible PPG is used for pulse wave monitoring

(A) Images (top left) and finite-element modeling (bottom left) results for PPG devices bent around glass cylinders; a binodal (chest and foot) deployment of skin-like wireless devices on neonate (right). Reproduced with permission.[111] Copyright 2019, AAAS.

(B) Health-tracking prototypes based on GQD PDs. Reproduced with permission.[113] Copyright 2019, AAAS.

(C) Schematic of the OPO sensor with the 8-shaped OPD.

(D) Cross-sectional view of ray diagrams: illustration (left) and optical simulation results (right) for the case where the substrate (PET) is directly optically coupled to the skin (top) and not directly optically coupled to the skin due to the presence of air gap between the substrate and the skin (bottom).

(E) Comparison of the power consumption of red and green light sources of oximetry sensors. Reproduced with permission.[114] Copyright 2018, AAAS.

(F) Schematic of the device structure of the flexible OPT (left); cuffless systolic blood pressure (SBP) and diastolic blood pressure (DBP) calculated from the hPPG-ECG, cPPG-ECG, and the cuff-based values as reference (right). Copyright 2017, Wiley. Used with permission from Xu et al.[115]

(G) Fully stretchable optoelectronic sensors based on colloidal quantum dots for sensing PPG signal. Reproduced with permission.[116] Copyright 2017, American Chemical Society.

miniaturization and flexibility. The miniaturization development is mainly from the direction of micro-electromechanical system (MEMS) production. For example, Wang's team used silicon-based materials to fabricate double-beam-block micro-structures (Figure 6A),[117] bat-shaped (Figure 6B),[118] and T-shaped (Figure 6C)[119] of a MEMS heart sound sensor (Figure 6D). The signal-to-noise ratio (Figure 6E) of the device made by the authors using a bat-shaped MEMS sensor was higher than that of a commercial sensor from 3M. To solve the limitation that the heart sound sensor cannot be in motion and worn on a hairy area, as shown in Figure 6F, Firat Güder and co-workers[120] made an acoustic coupling module. This acoustic coupling module used a 3D printed PLA (polylactic acid) mold to produce a water-silicone

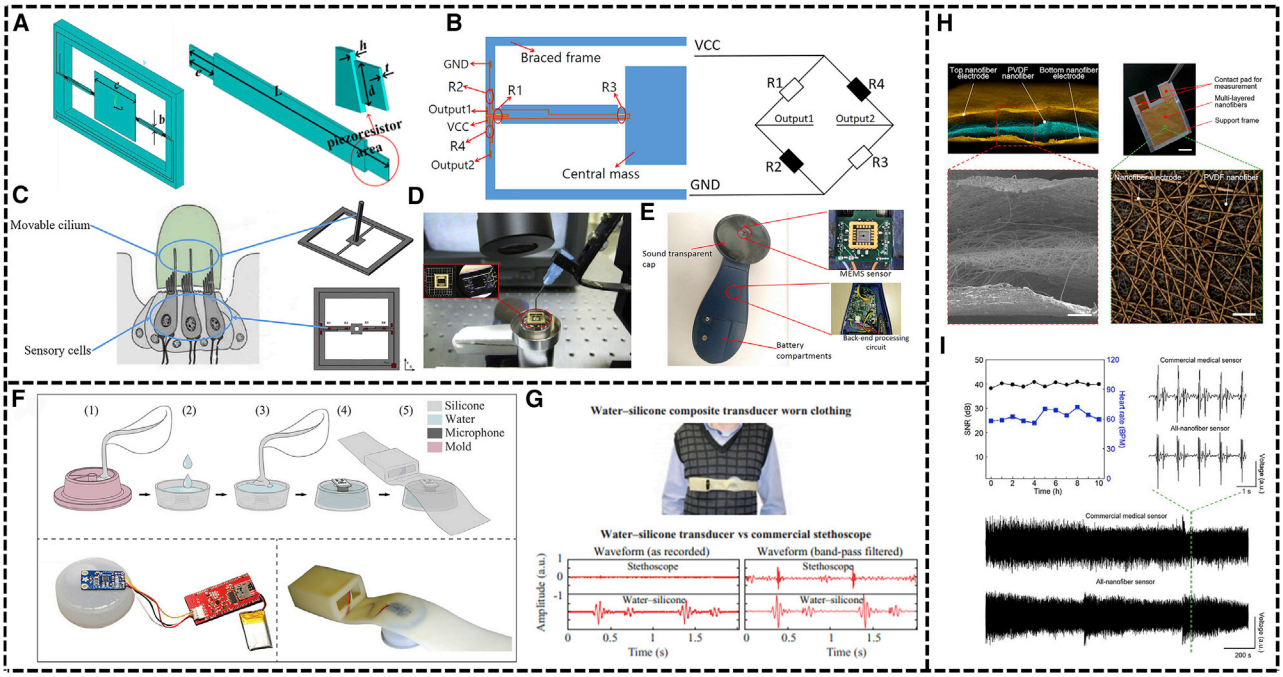

Figure 6. Wearable sensors are used for PCG

(A) The sensitive microstructure of the MEMS electronic heart sound sensor (left) and schematic of the cantilever beam (right). Reproduced with permission.[117] Copyright 2016, MDPI.

(B) Resistances distribution of Wheatstone bridge.

(C) T-type sensitive microstructure model.

(D) T-type MEMS heart sound sensor chip.

(E) The overall packaging of the bat-shape MEMS electronic stethoscope. Adapted from Wang et al.[118] and Pei et al.[119] with permission from Elsevier.

(F) Fabrication steps of the water–silicone composite transducer and the photograph of the device.

(G) Testing with healthy human volunteers (top) and the recorded sounds from the body with the water–silicone composite transducer versus commercial stethoscope (left bottom), after bandpass filtering with a Butterworth filter (passband 20–150 Hz) (right bottom). Copyright 2020, Wiley. Used with permission from Cotur et al.[120]

(H) Ultrasensitive all-nanofiber mechanoacoustic sensor, schematic (top left), the image of the sensor obtained by SEM (bottom left), optical photograph of the sensor (top right), surface 3D microscopic image of the sensor.

(I) SNR and heart rate in BPM during the 10-h experimental period (left top); comparison of the heart signals measured by a commercial cardiac microphone and an all-nanofiber sensor (bottom); a magnified version of the signals (top right). Reproduced with permission.[121] Copyright 2020, PNAS.

composite acoustic transducer. This transducer combined with a commercially available microphone could be worn directly on the waist to record heartbeat signals. The detected heart sound signals were superior to those collected by conventional stethoscopes (Figure 6G). Similarly, in terms of flexibility, Takao Someya's team[121] produced an all-nanofiber mechanical acoustic sensor with high air permeability sensitivity by electrospinning process (Figure 6H). The signal-to-noise ratio of the signal collected by this sensor reached 40.9 dB (Figure 6I).

The research work of flexible sensors for heart sound signals is relatively limited, and most of them are concentrated on micro-electromechanics. Since the heart sound signal is relatively weak and susceptible to noise interference, there are still great challenges in the sensitivity and anti-interference ability of the flexible sensor for heart sound signal monitoring in the future.

ECG

ECG signal is a typical electrophysiological (EP) signal that can reflect CVD and is most commonly used in clinical practice. Traditionally, a conductive gel is applied

to the body to reduce the interfacial impedance and improve the signal-to-noise ratio of the ECG signal when measured using an Ag/AgCl electrode. Since conductive gel may cause skin allergies and the electrodes are not flexible and cannot be attached to human skin well, researchers are beginning to study some flexible dry electrodes to replace the traditional ones. The basic design idea of these electrodes is based on two points: use of flexible conductive materials such as AgNWs,[122,123] Au,[124–126] graphene,[127–129] conductive polymers,[130] etc., and different structures designed to make the electrodes flexible and breathable and to have a high signal-to-noise ratio.

From the material point of view shown in Figure 7A, Bao's team[131] developed a flexible self-healing material, PDMS–MPU0.4–IU0.6, which forms a cross-linked network with strong (4,4′-methylenebis(phenyl urea) unit, MPU) and weak (isophorone bisurea unit, IU) dynamic bonding units incorporated into a PDMS backbone. This material was compounded with CNTs or AgNWs to obtain a flexible electrode with self-healing capability, and this material was used to make a stress sensor and a flexible light-emitting capacitor to verify a fully flexible system, respectively. To make the flexible electrode have the function of anti-epidermal grease, He et al.[125] grafted zwitterionic poly(2-methacryl-oyloxyethyl, methacryloyl-oxyethyl, or meth-acryloyloxyethyl phosphorylcholine) (PMPC) brush on the gold-plated PDMS. In this way, long-term use could be achieved by simple washing (Figure 7B). This grafted PMPC electrode did not lose signal information before and after washing compared to the ungrafted electrode. Aiming at wearable electronic devices that cannot properly adhere to the skin during exercise and are susceptible to motion artifacts, Ershad et al.[132] developed three types of electronic inks. Among them, Ag flakes/poly(3,4-ethylenedioxythiophene)-poly(styrenesulfonate) (Ag-PEDOT:PSS) composite was used as a conductive ink, and poly(3-hexylthiophene-2,5-diyl) nanofibrils (P3HT-NF) was used as a semiconducting ink. The gel was used as a dielectric ink. By using these three inks, a ballpoint pen was produced to draw ultra-conformal drawn-on-skin (DoS) electronics (Figure 7C) including strain sensors, thin film transistors, hydration sensors, temperature sensors, heaters, and electrophysiological sensors on the skin. The electrode monitoring ECG made in this way will not be affected by motion artifacts (Figure 7D). From the perspective of high conductivity, flexibility, and air permeability, Fan et al. used a facile in situ nonequilibrium fabrication process to produce a stretchable epidermal electrode (SEE) composed of polyurethane (PU) nanofibers and multilayer AgNWs (Figure 7E).[133] This SEE had excellent mechanical conformability and permeability to gases and liquids.

From the perspective of structural design, John's team did a series of work starting from the direction of the pattern structure. They chose a filamentary serpentine (FS) structure (Figure 7F) to fabricate a conformal epidermal electronic system (EES) that could integrate temperature sensing and tensile resistance sensing, as well as cardiac sensing.[126] Then, the processing circuit in the integrated circuit chip was connected by this wiring pattern, and the organic flexible material was used for packaging to achieve flexibility (Figure 7G).[134] Later, the pioneering method was applied to solve the multi-modal wireless signal detection in the intensive care units of infants or premature infants (Figure 7H) to replace traditional wired monitoring equipment.[111,112]

Flexible sensing was used in many research studies on the monitoring of ECG signals. ECG signals are also susceptible to environmental interference, so the electrodes are required to have extremely low impedance. However, there are still

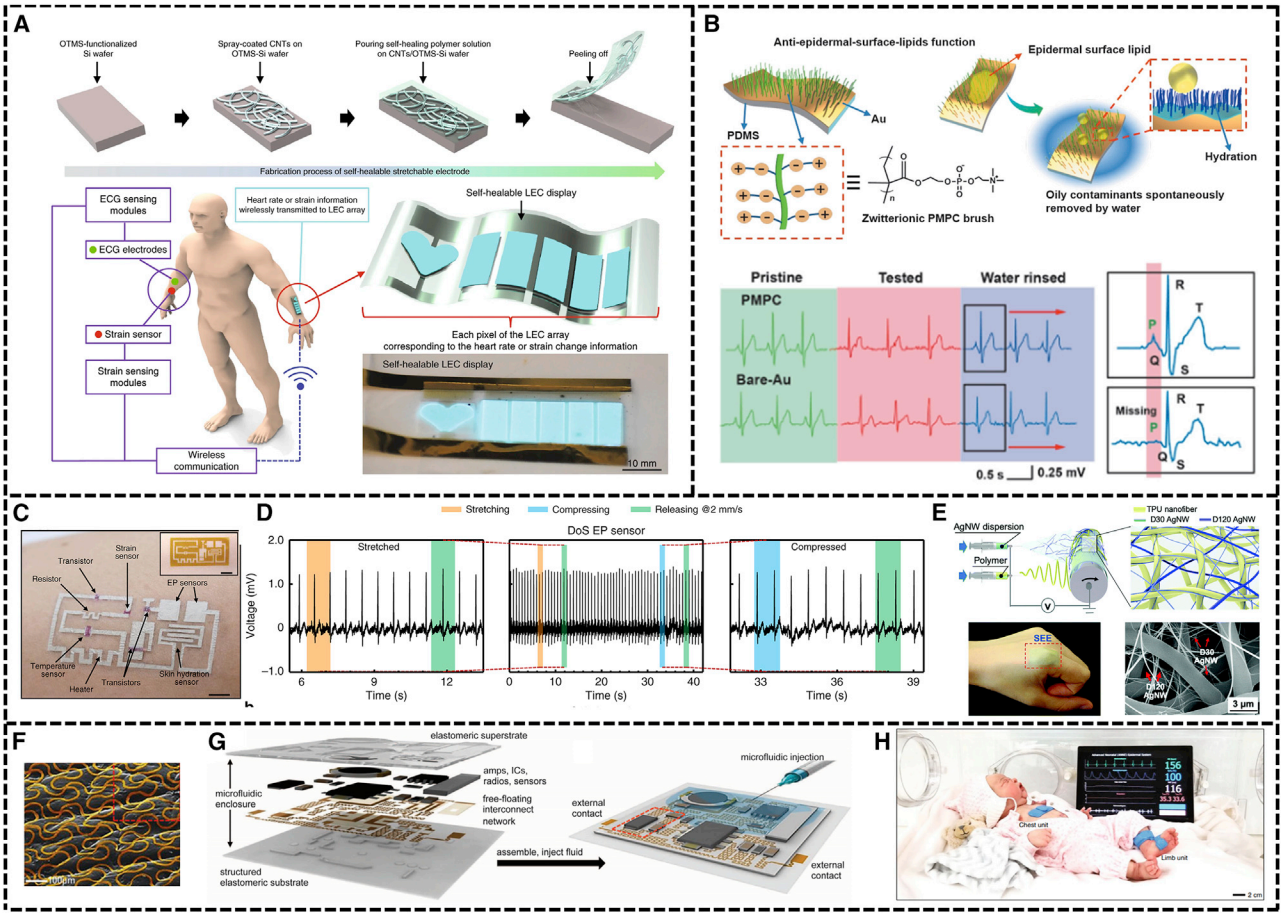

Figure 7. Flexible electrodes are used for ECG

(A) Schematic illustration of the fabrication process for the self-healable stretchable electrode (top); overview of the system with sensors wirelessly communicating values to the display (bottom).[131] Copyright 2018, Springer Nature.

(B) Configuration of the designed electrode (left top) and the water-enabled oil-cleaning effect (right top); the ECG signals evolution of both PMPC-grafted and bare Au/PDMS electrodes after tested being by epidermal surface lipids and rinsed by water (bottom). Copyright 2020, Wiley. Used with permission from He et al.[125]

(C) An example DoS integrated system.

(D) Recorded ECG signals (middle) from the DoS EP sensors during local stretching/releasing cycle (left) and compressing/releasing cycle (right).[132] Copyright 2020, Springer Nature.

(E) Fabrication and structure of the stretchable epidermal electrode (SEE).

(F) Colorized SEM image of an EES that uses FS structures (gold). Copyright 2013, Wiley. Used with permission from Yeo et al.[126]

(G) Illustration of the system. Reproduced with permission.[134] Copyright 2014, AAAS.

(H) Photograph of the chest and limb units on a model of a neonate in a NICU isolette.[112] Copyright 2020, Springer Nature.

certain challenges for the combination of the flexible electrode and the entire device. In the future, as silicon-based electronics with a relatively large modulus are converted into flexible components with a relatively small modulus, the applicability of wearable ECG monitoring will be greatly improved.

SCG/BCG and ACG

In addition to the above-mentioned more common signals that can reflect the cardiovascular status, SCG/BCG and ACG signals can also reflect the cardiovascular status of the human body. The SCG signal refers to the recording of chest wall vibration caused by the heart, the BCG is the recording of the body's reaction force when the heart injects blood into the blood vessels, and the ACG is a graphical

representation of the low-frequency vibration caused by the apical beats recorded at the apical part of the heart. In the past, research on them was mainly carried out from the aspects of instruments and algorithms.[135,136] With the development of flexible electronics and integrated circuits, the research direction has expanded, which has greatly promoted the development of CVD monitoring.

The monitoring of SCG signals is mostly recorded by three-axis acceleration.[137] As shown in Figure 8A, John's team[138] integrated accelerometers and capacitive electrodes into a soft, conformal-like device to record SCG and ECG signals (Figure 8B). In addition to continuously monitoring the blood flow of the left ventricular assist device (LVAD) pump speed, this device can also be used for voice recognition. In addition, Gupta et al.[139] (Figure 8C) applied a unique high-precision fabrication technique, namely high aspect-ratio combined poly- and single-crystal silicon micromachining technology (HARPSS), to fabricate accelerometer contact microphones (ACM) (Figure 8D) that can monitor SCG (Figure 8E), cardiopulmonary sounds, respiratory rate, heart rate, body movement, and position. The multimodal data sensed by this integrated MEMS sensor provided multi-dimensional health data for the calculation of HRV and inter-beat intervals (IBIs), which can monitor the human body better. To solve the non-stretchable characteristics of SCG based on rigid accelerometers, Lu's team[140] selected PVDF as the SCG sensing material and used the cut-and-paste fabrication method to simply and quickly fabricate a soft electro-mechano-acoustic cardiovascular (EMAC) electronic tattoos (e-tattoos).

For ACG signals, You et al.[141] chose Au nanoparticles and elastomer PDMS to make a stretchable electronic skin ACG strain sensor (Figure 8G). This kind of sensor was made of a dry rubbing process with high sensitivity under small strain and excellent stability under large strain. Since ACG is a vibration produced by apex beats, it can also be measured with a pressure transducer. The sensor made in this way can measure not only ACG signal but also pulse wave signals. For example, Guo et al.[102] used the anodized aluminum template method to make a low-cost flexible capacitive pressure sensor (Figure 8H) for ACG detection (Figure 8I). This sensor selected P(VDF-TrFE) as the dielectric layer with high sensitivity (0.35 kPa^{-1}), wide operating range (4 Pa to 25 kPa), short response time, and excellent durability.

There are relatively few studies on flexible sensors used in SCG/BCG and ACG signal monitoring compared to pulse wave and ECG signals. In monitoring SCG/BCG and ACG signals, there are still relatively big challenges in terms of sensitivity. With the deepening of research on signals and CVD, the future flexible sensor monitoring of SCG/BCG and ACG signals will promote the prevention of CVD.

Other types

Besides body surface signals and electrophysiological signals caused by heartbeat, researchers also monitor the human body through methods such as temperature sensing, optical fiber sensing, and organic triode.[142] Gao et al.[143] used thermochromic liquid crystal (TLC) materials to make epidermal thermochromic liquid crystals (e-TLCs) (Figure 9A) to obtain a map of blood vessel temperatures. The accuracy of the sensor has reached millikelvin precision ($\pm$50 mK). The epidermal photonic systems represented by the e-TLC device provide a powerful potential for characterizing the skin, which in turn provides important parameters for determining cardiovascular health and physiological status. In addition, Webb et al.[144] reported a ring temperature measurement device made of Cr/Ag wires. In the middle of the device, there was a thermal actuator that served as a heating element, and a total of 14 thermometers (Figure 9B) were placed at 45° intervals around two circles on the sides to

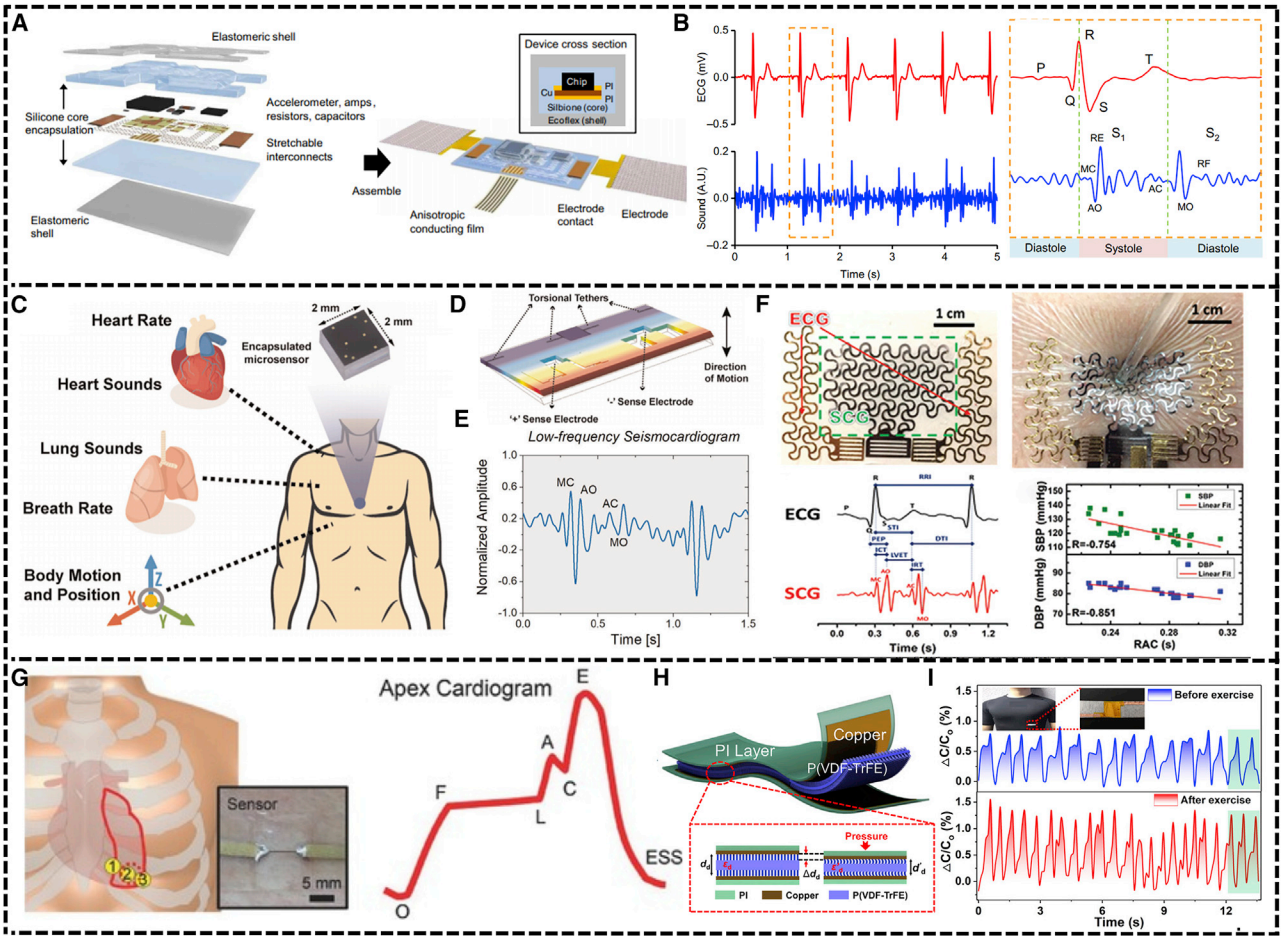

Figure 8. Flexible sensors are used for SCG/BCG or ACG

(A) Schematic illustration of an epidermal mechano-acoustic–electrophysiological measurement device.

(B) Plot of ECG (top) and heart sound (bottom) signals measured simultaneously. Reproduced with permission.[138] Copyright 2016, AAAS.

(C) Hermetically sealed sensor with nanogaps for cardiopulmonary health monitoring.

(D) COMSOL multiphysics simulation.

(E) Time domain plot of measured SCG signal.[139] Copyright 2020, Springer Nature.

(F) Stretchable EMAC sensing tattoo for continuous BP estimation. Copyright 2019, Wiley. Used with permission from Ha et al.[140]

(G) Schematics of ACG measurement and sensor system, and the typical ACG contour (left), ACG profiles of the sensor (right). Copyright 2016, Wiley. Used with permission from You et al.[141]

(H) Assembly of the capacitive pressure sensor by incorporating copper as the electrodes and PI as the encapsulation layers.

(I) Obtained capacitance responses corresponding to the ACG waveforms for the situation before and after exercise. Reproduced with permission.[102] Copyright 2019, American Chemical Society.

obtain the relationship between temperature and blood flow velocity. This device could measure blood flow in a deeper position than traditional methods (Figure 9C).

Different from the conventional principle of measuring pulse waves, as shown in Figure 9D, Fu et al.[145] used structured Ag particles and PDMS to make piezothermic transduction. The sensor consists of two parts: an Ag/PDMS composite material on top and a Pt/Cr central and peripheral band on the bottom. The sensor is based on a characteristic of this composite, that its thermal conductivity can change with pressure. The authors used a constant temperature difference (CTD) feedback circuit to measure the change in resistance due to temperature change and ultimately the change in voltage. Because the commonly used electronic components for pulse measurement were subject to electromagnetic interference, Wang et al.[146] made

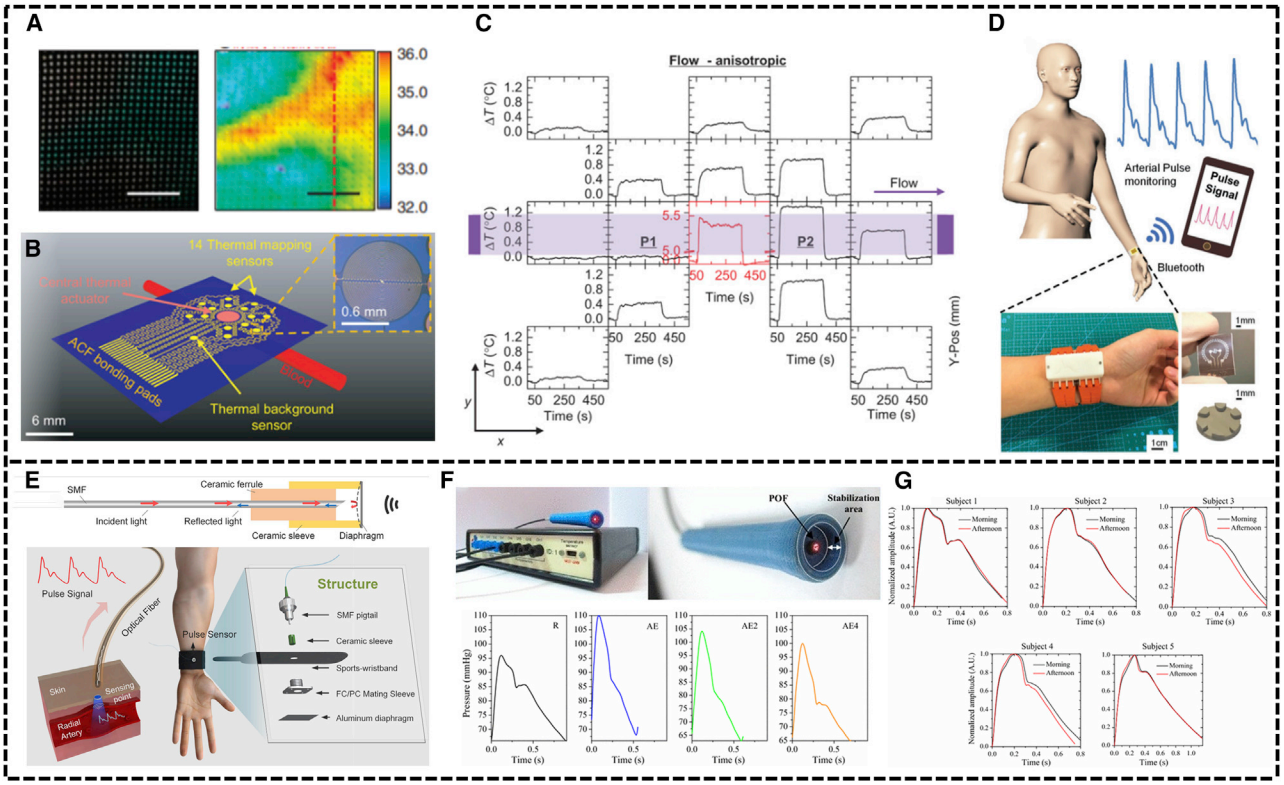

Figure 9. Other types of sensors are used for CVD

(A) Images of an e-TLC device (left); three-dimensional rendering of the temperature distribution (right).[143] Copyright 2014, Springer Nature.

(B) Schematic illustration of the device layout.

(C) Raw data from a device applied to an area above a large vessel. Reproduced with permission.[144] Copyright 2015, AAAS.

(D) Configuration of the pulse monitoring system. Copyright 2019, Wiley. Used with permission from Fu et al.[145]

(E) Schematic diagram of optical fiber pulse sensor (top), structural design of wearable pulse sensor (bottom). Copyright 2019, Wiley. Used with permission from Wang et al.[146]

(F) Optical fiber pen-like probes based on intensity modulation (top), and central arterial pressures profiles of subject 1 in the resting position (R), immediately after exercise (AE), and 2 and 4 min after exercise (AE2 and AE4, respectively) (bottom).

(G) Comparison of the average pulses of morning and afternoon for each subject.[147] Copyright 2016, Springer Nature.

an optical fiber sensor using aluminum film as a sensitive component to measure pulse waves through a coherent phase detection method (Figure 9E). Leitão et al.[147] reported a single fiber Bragg grating (FBG) sensing device. Plastic optical fiber (POF) was used in this device, and the sensor was a pen-like probe. It was used to measure pulse waves 2 and 4 min after resting and exercise (Figure 9F). Mean carotid arteries were also measured in the morning and afternoon over the course of a week in five subjects, and differences in HR were found to only alter diastole (Figure 9G).

Here, we introduced temperature signal and some special methods using the coherent phase principle of light to obtain cardiovascular status. In addition to some of the methods described above, there are also signals and parameters such as blood glucose to obtain the cardiovascular status of the human body. Different methods to obtain cardiovascular status have their own advantages and disadvantages. In the future, multiple methods and dimensions to assess cardiovascular status will greatly increase the accuracy of the assessment. The more information, the more accurately the cardiovascular status of the human body can be obtained.

CONCLUSIONS AND OUTLOOK

In this review, we focused on five types of signals that can reflect CVD and related wearable flexible sensors and devices. In terms of pulse wave, some time-domain parameters that can reflect heart function and peripheral vascular conditions were summarized. Since different types of signals could be generated during the heartbeat, such as pulse wave, PCG, ECG, and other signals, it is particularly important to collect these signals. In the design and research of flexible sensors, the sensitivity and sensing range were continuously expanded mainly from the selection of materials and structural design. The combination of multi-modal sensing mechanism and flexible sensing brought more choices for cardiovascular health monitoring. For example, in the flexible sensors monitoring the ECG signals, the integrated circuit and flexible material were combined to construct the entire practical device, which brought certain inspiration and ideas for the commercialization of flexible sensors. In addition, the vigorous development of MEMS technology would be more conducive to wearable devices for CVD monitoring.

Although the conformal structural design and material design that fit the skin have brought opportunities for wearable medical care, the prevention of CVD still requires continuous research and exploration. Due to the diversity of the information brought by the heart and blood in CVD, the conditions of the heart and blood vessels can be reflected through pulse waves, ECG, PCG, SCG/BCG, and ACG. Nowadays, the design of flexible sensing mainly focuses on pulse waves and ECG. There are few studies on flexible sensing materials in the areas of PCG, SCG/BCG, and ACG. Most of the sensors that have been reported can acquire only one signal. Although there are some that can detect two kinds of signals, the acquirde signals are more affected by noise, and basically stay in the laboratory. Starting from basic materials and devices, the new constructed wearable devices can be more conformable to human skin than commercial ones. In addition, the complexity of CVD requires that the target of flexible sensor monitoring is multi-modal signals. In the future, research on monitoring human multi-modal signals by flexible wearable devices will start from the materials of the sensor, to the device, and finally to the signal analysis. Combined AIoT (artificial intelligence and Internet of Things) technology will be more conducive to the early prevention of CVD, making human cardiovascular health monitoring more accurate and personalized and bringing benefits to human life and health.

ACKNOWLEDGMENTS

This work was supported by the National Natural Science Foundation of China (grants 51932002, 51903087, 51772106, and 31771080), the Science and Technology Program of Guangzhou (grant 202002030308), the Science and Technology Innovation Team Project of Foshan (grant 2018IT100101), and Sino-Singapore International Joint Research Institute (grant 203-A018004).

AUTHOR CONTRIBUTIONS

J.L. contributed to literature collection and analysis and manuscript writing and revising. R.F., X.Z., P.Y., G.T., W.L., and H.Z. contributed to manuscript revision. Y.L., L.Z., and C.N. contributed to project design and financial support.

DECLARATION OF INTERESTS

The authors declare no competing interests.

REFERENCES

1. The Writing Committee of the Report on Cardiovascular Health and Diseases in China (2020). Report on cardiovascular health and diseases in China 2019: an updated summary. Chin Circ J. *35*, 833–854.
2. Timmis, A., Townsend, N., Gale, C.P., Torbica, A., Lettino, M., Petersen, S.E., Mossialos, E.A., Maggioni, A.P., Kazakiewicz, D., May, H.T., et al.; European Society of Cardiology (2020). European Society of Cardiology: Cardiovascular disease statistics 2019. Eur. Heart J. *41*, 12–85.
3. Andreu-Perez, J., Leff, D.R., Ip, H.M., and Yang, G.Z. (2015). From wearable sensors to smart implants—toward pervasive and personalized healthcare. IEEE Trans. Biomed. Eng. *62*, 2750–2762.
4. Wang, Z., Cong, Y., and Fu, J. (2020). Stretchable and tough conductive hydrogels for flexible pressure and strain sensors. J. Mater. Chem. B Mater. Biol. Med. *8*, 3437–3459.
5. Vilela, D., Romeo, A., and Sánchez, S. (2016). Flexible sensors for biomedical technology. Lab Chip *16*, 402–408.
6. Mishra, S., Unnikrishnan, L., Nayak, S.K., and Mohanty, S. (2019). Advances in piezoelectric polymer composites for energy harvesting applications: a systematic review. Macromol. Mater. Eng. *304*, 1800463.
7. Lim, H.R., Kim, H.S., Qazi, R., Kwon, Y.T., Jeong, J.W., and Yeo, W.H. (2020). Advanced soft materials, sensor integrations, and applications of wearable flexible hybrid electronics in healthcare, energy, and environment. Adv. Mater. *32*, e1901924.
8. Lee, E.K., Kim, M.K., and Lee, C.H. (2019). Skin-mountable biosensors and therapeutics: a review. Annu. Rev. Biomed. Eng. *21*, 299–323.
9. Kim, D.C., Shim, H.J., Lee, W., Koo, J.H., and Kim, D.H. (2020). Material-based approaches for the fabrication of stretchable electronics. Adv. Mater. *32*, e1902743.
10. Hong, Y.J., Jeong, H., Cho, K.W., Lu, N., and Kim, D.H. (2019). Wearable and implantable devices for cardiovascular healthcare: from monitoring to therapy based on flexible and stretchable electronics. Adv. Funct. Mater. *29*, 1808247.
11. Li, J., Bao, R., Tao, J., Peng, Y., and Pan, C. (2018). Recent progress in flexible pressure sensor arrays: from design to applications. J. Mater. Chem. C Mater. Opt. Electron. Devices *6*, 11878–11892.
12. Chen, Y., Zhang, Y., Liang, Z., Cao, Y., Han, Z., and Feng, X. (2020). Flexible inorganic bioelectronics. Flexible Electron *4*, 1–20.
13. Chen, S., Qi, J., Fan, S., Qiao, Z., Yeo, J.C., and Lim, C.T. (2021). Flexible wearable sensors for cardiovascular health monitoring. Adv. Healthc. Mater *2021*, e2100116.
14. Koydemir, H.C., and Ozcan, A. (2018). Wearable and implantable sensors for biomedical applications. Annu. Rev. Anal. Chem. (Palo Alto, Calif.) *11*, 127–146.
15. Yang, G., Pang, G., Pang, Z., Gu, Y., Mantysalo, M., and Yang, H. (2019). Non-invasive flexible and stretchable wearable sensors with nano-based enhancement for chronic disease care. IEEE Rev. Biomed. Eng. *12*, 34–71.
16. O'Rourke, M.F., Pauca, A., and Jiang, X.-J. (2001). Pulse wave analysis. Br. J. Clin. Pharmacol. *51*, 507–522.
17. Davies, J.I., and Struthers, A.D. (2003). Pulse wave analysis and pulse wave velocity: a critical review of their strengths and weaknesses. J. Hypertens. *21*, 463–472.
18. Vlachopoulos, C., O'Rourke, M., and Nichols, W.W. (2011). McDonald's Blood Flow in Arteries: Theoretical, Experimental and Clinical Principles (CRC Press).
19. Mitchell, G.F. (2006). Triangulating the peaks of arterial pressure. Hypertension *48*, 543–545.
20. Swamy, G., Olivier, N.B., and Mukkamala, R. (2010). Calculation of forward and backward arterial waves by analysis of two pressure waveforms. IEEE Trans. Biomed. Eng. *57*, 2833–2839.
21. Hou, J., Zhang, Y., Zhang, S., Geng, X., Zhang, J., Chen, C., and Zhang, H. (2020). A novel angle extremum maximum method for recognition of pulse wave feature points. Comput. Methods Programs Biomed. *189*, 105321.
22. Korpas, D., Hálek, J., and Dolezal, L. (2009). Parameters describing the pulse wave. Physiol. Res. *58*, 473–479.
23. Proença, M., Renevey, P., Braun, F., Bonnier, G., Delgado-Gonzalo, R., Lemkaddem, A., Verjus, C., Ferrario, D., and Lemay, M. (2019). The Handbook of Cuffless Blood Pressure Monitoring: A Practical Guide for Clinicians, Researchers, and Engineers, J. Solà and R. Delgado-Gonzalo, eds. (Cham: Springer International Publishing), pp. 107–137.
24. Hansen, P.B., Luisada, A.A., Miletich, D.J., and Albrecht, R.F. (1989). Phonocardiography as a monitor of cardiac performance during anesthesia. Anesth. Analg. *68*, 385–387.
25. Durand, L.-G., Langlois, Y.-E., Lanthier, T., Chiarella, R., Coppens, P., Carioto, S., and Bertrand-Bradley, S. (1990). Spectral analysis and acoustic transmission of mitral and aortic valve closure sounds in dogs. Part 1. Modelling the heart/thorax acoustic system. Med. Biol. Eng. Comput. *28*, 269–277.
26. Saul, J.P. (1990). Beat-to-beat variations of heart rate reflect modulation of cardiac autonomic outflow. Physiology (Bethesda) *5*, 32–37.
27. Kouhyar Tavakolian, A.P.B. (2010). Brandon Ngai, Bozena Kaminska. Computing in Cardiology*Volume 37* (Belfast: IEEE), pp. 1055–1058.
28. Sørensen, K., Schmidt, S.E., Jensen, A.S., Søgaard, P., and Struijk, J.J. (2018). Definition of fiducial points in the normal seismocardiogram. Sci. Rep. *8*, 15455.
29. Akhbardeh, A., Junnila, S., Koivuluoma, M., Koivistoinen, T., and Varri, A. (2005). IEEE/ASME International Conference on Advanced Intelligent Mechatronics, Monterey, 2005 (IEEE), pp. 676–681.
30. Xia, X., Zhang, X., Serpe, M.J., and Zhang, Q. (2019). Microgel-based devices as wearable capacitive electronic skins for monitoring cardiovascular risks. Adv. Mater. Technol. *5*, 1900818.
31. Khang, D.-Y., Jiang, H., Huang, Y., and Rogers, J.A. (2006). A stretchable form of single-crystal silicon for high-performance electronics on rubber substrates. Science *311*, 208–212.
32. Hoque, N.A., Thakur, P., Biswas, P., Saikh, M.M., Roy, S., Bagchi, B., Das, S., and Ray, P.P. (2018). Biowaste crab shell-extracted chitin nanofiber-based superior piezoelectric nanogenerator. J. Mater. Chem. A Mater. Energy Sustain. *6*, 13848–13858.
33. Maity, K., Garain, S., Henkel, K., Schmeißer, D., and Mandal, D. (2018). Natural sugar-assisted, chemically reinforced, highly durable piezoorganic nanogenerator with superior power density for self-powered wearable electronics. ACS Appl. Mater. Interfaces *10*, 44018–44032.
34. Wang, W., Zheng, Y., Jin, X., Sun, Y., Lu, B., Wang, H., Fang, J., Shao, H., and Lin, T. (2019). Unexpectedly high piezoelectricity of electrospun polyacrylonitrile nanofiber membranes. Nano Energy *56*, 588–594.
35. Chen, X., Li, X., Shao, J., An, N., Tian, H., Wang, C., Han, T., Wang, L., and Lu, B. (2017). High-performance piezoelectric nanogenerators with imprinted P(VDF-TrFE)/$BaTiO_3$ nanocomposite micropillars for self-powered flexible sensors. Small *13*, 1604245.
36. Li, H., Zhang, W., Ding, Q., Jin, X., Ke, Q., Li, Z., Wang, D., and Huang, C. (2019). Facile strategy for fabrication of flexible, breathable, and washable piezoelectric sensors via welding of nanofibers with multiwalled carbon nanotubes (MWCNTs). ACS Appl. Mater. Interfaces *11*, 38023–38030.
37. Zhang, Z., Chen, L., Yang, X., Li, T., Chen, X., Li, X., Zhao, T., and Zhang, J. (2018). Enhanced flexible piezoelectric sensor by the integration of P(VDF-TrFE)/AgNWs film with a-IGZO TFT. IEEE Electron Device Lett. *40*, 111–114.
38. Huynh, T.H., Jafari, R., and Chung, W.Y. (2019). Noninvasive cuffless blood pressure estimation using pulse transit time and impedance plethysmography. IEEE Trans. Biomed. Eng. *66*, 967–976.
39. Zhang, Y., and Kim, W.S. (2014). Highly sensitive flexible printed accelerometer system for monitoring vital signs. Soft Robotics *1*, 132–135.
40. Shi, X., Wang, H., Xie, X., Xue, Q., Zhang, J., Kang, S., Wang, C., Liang, J., and Chen, Y. (2019). Bioinspired ultrasensitive and stretchable MXene-based strain sensor via nacre-mimetic microscale "brick-and-mortar" architecture. ACS Nano *13*, 649–659.

41. Ji, B., Zhou, Q., Wu, J., Gao, Y., Wen, W., and Zhou, B. (2020). Synergistic optimization toward the sensitivity and linearity of flexible pressure sensor via double conductive layer and porous microdome array. ACS Appl. Mater. Interfaces *12*, 31021–31035.

42. Shi, X., Liu, S., Sun, Y., Liang, J., and Chen, Y. (2018). Lowering internal friction of 0D-1D-2D ternary nanocomposite-based strain sensor by fullerene to boost the sensing performance. Adv. Funct. Mater. *28*, 1800850.

43. Li, X., Fan, Y.J., Li, H.Y., Cao, J.W., Xiao, Y.C., Wang, Y., Liang, F., Wang, H.L., Jiang, Y., Wang, Z.L., and Zhu, G. (2020). Ultracomfortable hierarchical nanonetwork for highly sensitive pressure sensor. ACS Nano *14*, 9605–9612.

44. Pang, Y., Zhang, K., Yang, Z., Jiang, S., Ju, Z., Li, Y., Wang, X., Wang, D., Jian, M., Zhang, Y., et al. (2018). Epidermis microstructure inspired graphene pressure sensor with random distributed spinosum for high sensitivity and large linearity. ACS Nano *12*, 2346–2354.

45. Yang, T., Jiang, X., Zhong, Y., Zhao, X., Lin, S., Li, J., Li, X., Xu, J., Li, Z., and Zhu, H. (2017). A wearable and highly sensitive graphene strain sensor for precise home-based pulse wave monitoring. ACS Sens. *2*, 967–974.

46. He, J., Xiao, P., Lu, W., Shi, J., Zhang, L., Liang, Y., Pan, C., Kuo, S.-W., and Chen, T. (2019). A universal high accuracy wearable pulse monitoring system via high sensitivity and large linearity graphene pressure sensor. Nano Energy *59*, 422–433.

47. Zang, S., Wang, Q., Mi, Q., Zhang, J., and Ren, X. (2017). A facile, precise radial artery pulse sensor based on stretchable graphene-coated fiber. Sens. Actuators A Phys. *267*, 532–537.

48. Park, J., Kim, M., Lee, Y., Lee, H.S., and Ko, H. (2015). Fingertip skin-inspired microstructured ferroelectric skins discriminate static/dynamic pressure and temperature stimuli. Sci. Adv. *1*, e1500661.

49. Liu, Y., Meng, F., Zhou, Y., Mugo, S.M., and Zhang, Q. (2019). Graphene oxide films prepared using gelatin nanofibers as wearable sensors for monitoring cardiovascular health. Adv. Mater. Technol. *4*, 1900540.

50. Qiao, Y., Wang, Y., Tian, H., Li, M., Jian, J., Wei, Y., Tian, Y., Wang, D.Y., Pang, Y., Geng, X., et al. (2018). Multilayer graphene epidermal electronic skin. ACS Nano *12*, 8839–8846.

51. Wu, X., Hou, K., Huang, J., Wang, J., and Yang, S. (2018). Graphene-based cellular materials with extremely low density and high pressure sensitivity based on self-assembled graphene oxide liquid crystals. J. Mater. Chem. C Mater. Opt. Electron. Devices *6*, 8717–8725.

52. Chen, Z., Wang, Z., Li, X., Lin, Y., Luo, N., Long, M., Zhao, N., and Xu, J.B. (2017). Flexible piezoelectric-induced pressure sensors for static measurements based on nanowires/graphene heterostructures. ACS Nano *11*, 4507–4513.

53. Wu, Q., Qiao, Y., Guo, R., Naveed, S., Hirtz, T., Li, X., Fu, Y., Wei, Y., Deng, G., Yang, Y., et al. (2020). Triode-mimicking graphene pressure sensor with positive resistance variation for physiology and motion monitoring. ACS Nano *14*, 10104–10114.

54. Guo, Q., Zhang, X., Zhao, F., Song, Q., Su, G., Tan, Y., Tao, Q., Zhou, T., Yu, Y., Zhou, Z., and Lu, C. (2020). Protein-inspired self-healable Ti_3C_2 MXenes/Rubber-based supramolecular elastomer for intelligent sensing. ACS Nano *14*, 2788–2797.

55. Wu, X., Liao, H., Ma, D., Chao, M., Wang, Y., Jia, X., Wan, P., and Zhang, L. (2020). A wearable, self-adhesive, long-lastingly moist and healable epidermal sensor assembled from conductive MXene nanocomposites. J. Mater. Chem. C Mater. Opt. Electron. Devices *8*, 1788–1795.

56. Zhang, Y.-Z., Lee, K.H., Anjum, D.H., Sougrat, R., Jiang, Q., Kim, H., and Alshareef, H.N. (2018). MXenes stretch hydrogel sensor performance to new limits. Sci. Adv. *4*, eaat0098.

57. Yue, Y., Liu, N., Liu, W., Li, M., Ma, Y., Luo, C., Wang, S., Rao, J., Hu, X., Su, J., et al. (2018). 3D hybrid porous Mxene-sponge network and its application in piezoresistive sensor. Nano Energy *50*, 79–87.

58. Guo, Y., Zhong, M., Fang, Z., Wan, P., and Yu, G. (2019). A wearable transient pressure sensor made with MXene nanosheets for sensitive broad-range human-machine interfacing. Nano Lett. *19*, 1143–1150.

59. Cheng, Y., Ma, Y., Li, L., Zhu, M., Yue, Y., Liu, W., Wang, L., Jia, S., Li, C., Qi, T., et al. (2020). Bioinspired microspines for a high-performance spray $Ti_3C_2T_x$ MXene-based piezoresistive sensor. ACS Nano *14*, 2145–2155.

60. Yang, Y., Shi, L., Cao, Z., Wang, R., and Sun, J. (2019). Strain sensors with a high sensitivity and a wide sensing range based on a Ti3C2Tx(MXene) nanoparticle–nanosheet hybrid network. Adv. Funct. Mater. *29*, 1807882.

61. Wang, K., Lou, Z., Wang, L., Zhao, L., Zhao, S., Wang, D., Han, W., Jiang, K., and Shen, G. (2019). Bioinspired interlocked structure-induced high deformability for two-dimensional titanium carbide (MXene)/natural microcapsule-based flexible pressure sensors. ACS Nano *13*, 9139–9147.

62. Qin, R., Hu, M., Li, X., Yan, L., Wu, C., Liu, J., Gao, H., Shan, G., and Huang, W. (2020). A highly sensitive piezoresistive sensor based on MXenes and polyvinyl butyral with a wide detection limit and low power consumption. Nanoscale *12*, 17715–17724.

63. Miao, L., Wan, J., Song, Y., Guo, H., Chen, H., Cheng, X., and Zhang, H. (2019). Skin-inspired humidity and pressure sensor with a wrinkle-on-sponge structure. ACS Appl. Mater. Interfaces *11*, 39219–39227.

64. Liao, M., Wan, P., Wen, J., Gong, M., Wu, X., Wang, Y., Shi, R., and Zhang, L. (2017). Wearable, healable, and adhesive epidermal sensors assembled from mussel-inspired conductive hybrid hydrogel framework. Adv. Funct. Mater. *27*, 1703852.

65. Wang, X., Gu, Y., Xiong, Z., Cui, Z., and Zhang, T. (2014). Silk-molded flexible, ultrasensitive, and highly stable electronic skin for monitoring human physiological signals. Adv. Mater. *26*, 1336–1342.

66. Han, Z., Cheng, Z., Chen, Y., Li, B., Liang, Z., Li, H., Ma, Y., and Feng, X. (2019). Fabrication of highly pressure-sensitive, hydrophobic, and flexible 3D carbon nanofiber networks by electrospinning for human physiological signal monitoring. Nanoscale *11*, 5942–5950.

67. Wang, Z., Chen, J., Cong, Y., Zhang, H., Xu, T., Nie, L., and Fu, J. (2018). Ultrastretchable strain sensors and arrays with high sensitivity and linearity based on super tough conductive hydrogels. Chem. Mater. *30*, 8062–8069.

68. Choi, Y.W., Kang, D., Pikhitsa, P.V., Lee, T., Kim, S.M., Lee, G., Tahk, D., and Choi, M. (2017). Ultra-sensitive pressure sensor based on guided straight mechanical cracks. Sci. Rep. *7*, 40116.

69. Liu, Y.F., Liu, Q., Li, Y.Q., Huang, P., Yao, J.Y., Hu, N., and Fu, S.Y. (2020). Spider-inspired ultrasensitive flexible vibration sensor for multifunctional sensing. ACS Appl. Mater. Interfaces *12*, 30871–30881.

70. Xu, H., Xiang, J.X., Lu, Y.F., Zhang, M.K., Li, J.J., Gao, B.B., Zhao, Y.J., and Gu, Z.Z. (2018). Multifunctional wearable sensing devices based on functionalized graphene films for simultaneous monitoring of physiological signals and volatile organic compound biomarkers. ACS Appl. Mater. Interfaces *10*, 11785–11793.

71. Zhang, L., Hu, F., Zhu, S., Lin, Y., Meng, Z., Yu, R., and Liu, X.Y. (2020). Meso-reconstruction of wool keratin 3D "molecular springs" for tunable ultra-sensitive and highly recovery strain sensors. Small *16*, e2000128.

72. Wu, X., Li, Z., Wang, H., Huang, J., Wang, J., and Yang, S. (2019). Stretchable and self-healable electrical sensors with fingertip-like perception capability for surface texture discerning and biosignal monitoring. J. Mater. Chem. C Mater. Opt. Electron. Devices *7*, 9008–9017.

73. Wang, T., Zhang, Y., Liu, Q., Cheng, W., Wang, X., Pan, L., Xu, B., and Xu, H. (2018). A self-healable, highly stretchable, and solution processable conductive polymer composite for ultrasensitive strain and pressure sensing. Adv. Funct. Mater. *28*, 1705551.

74. Tsai, Y.J., Wang, C.M., Chang, T.S., Sutradhar, S., Chang, C.W., Chen, C.Y., Hsieh, C.H., and Liao, W.S. (2019). Multilayered Ag NP-PEDOT-paper composite device for human-machine interfacing. ACS Appl. Mater. Interfaces *11*, 10380–10388.

75. Yin, B., Liu, X., Gao, H., Fu, T., and Yao, J. (2018). Bioinspired and bristled microparticles for ultrasensitive pressure and strain sensors. Nat. Commun. *9*, 5161.

76. Han, Z., Li, H., Xiao, J., Song, H., Li, B., Cai, S., Chen, Y., Ma, Y., and Feng, X. (2019). Ultralow-cost, highly sensitive, and flexible pressure sensors based on carbon black and airlaid paper for wearable electronics. ACS Appl. Mater. Interfaces *11*, 33370–33379.

77. Tan, P., Zou, Y., Fan, Y., and Li, Z. (2020). Self-powered wearable electronics. Wearable Technologies. *1*, e5.

78. Pu-Chuan, T., Chao-Chao, Z., Yu-Bo, F., and Zhou, L. (2020). Research progress of self-powered flexible biomedical sensors. Wuli Xuebao *69*, 178704.

79. Fu, R., Tu, L., Zhou, Y., Fan, L., Zhang, F., Wang, Z., Xing, J., Chen, D., Deng, C., Tan, G., et al. (2019). A tough and self-powered hydrogel for artificial skin. Chem. Mater. *31*, 9850–9860.

80. Chu, Y., Zhong, J., Liu, H., Ma, Y., Liu, N., Song, Y., Liang, J., Shao, Z., Sun, Y., Dong, Y., et al. (2018). Human pulse diagnosis for medical assessments using a wearable piezoelectret sensing system. Adv. Funct. Mater. *28*, 1803413.

81. Li, T., Feng, Z.Q., Qu, M., Yan, K., Yuan, T., Gao, B., Wang, T., Dong, W., and Zheng, J. (2019). Core/shell piezoelectric nanofibers with spatial self-orientated β-phase nanocrystals for real-time micropressure monitoring of cardiovascular walls. ACS Nano *13*, 10062–10073.

82. Park, S.H., Lee, H.B., Yeon, S.M., Park, J., and Lee, N.K. (2016). Flexible and stretchable piezoelectric sensor with thickness-tunable configuration of electrospun nanofiber mat and elastomeric substrates. ACS Appl. Mater. Interfaces *8*, 24773–24781.

83. Chen, S., Wu, N., Lin, S., Duan, J., Xu, Z., Pan, Y., Zhang, H., Xu, Z., Huang, L., Hu, B., and Zhou, J. (2020). Hierarchical elastomer tuned self-powered pressure sensor for wearable multifunctional cardiovascular electronics. Nano Energy *70*, 104460.

84. Chen, J., Liu, H., Wang, W., Nabulsi, N., Zhao, W., Kim, J.Y., Kwon, M.K., and Ryou, J.H. (2019). High durable, biocompatible, and flexible piezoelectric pulse sensor using single-crystalline III-N thin film. Adv. Funct. Mater. *29*, 1903162.

85. Dagdeviren, C., Su, Y., Joe, P., Yona, R., Liu, Y., Kim, Y.S., Huang, Y., Damadoran, A.R., Xia, J., Martin, L.W., et al. (2014). Conformable amplified lead zirconate titanate sensors with enhanced piezoelectric response for cutaneous pressure monitoring. Nat. Commun. *5*, 4496.

86. Park, D.Y., Joe, D.J., Kim, D.H., Park, H., Han, J.H., Jeong, C.K., Park, H., Park, J.G., Joung, B., and Lee, K.J. (2017). Self-powered real-time arterial pulse monitoring using ultrathin epidermal piezoelectric sensors. Adv. Mater. *29*, 1702308.

87. Wang, C., Li, X., Hu, H., Zhang, L., Huang, Z., Lin, M., Zhang, Z., Yin, Z., Huang, B., Gong, H., et al. (2018). Monitoring of the central blood pressure waveform via a conformal ultrasonic device. Nat. Biomed. Eng. *2*, 687–695.

88. Ouyang, H., Tian, J., Sun, G., Zou, Y., Liu, Z., Li, H., Zhao, L., Shi, B., Fan, Y., Fan, Y., et al. (2017). Self-powered pulse sensor for antidiastole of cardiovascular disease. Adv. Mater. *29*, 1703456.

89. Peng, X., Dong, K., Ye, C., Jiang, Y., Zhai, S., Cheng, R., Liu, D., Gao, X., Wang, J., and Wang, Z.L. (2020). A breathable, biodegradable, antibacterial, and self-powered electronic skin based on all-nanofiber triboelectric nanogenerators. Sci. Adv. *6*, eaba9624.

90. Zou, Y., Liao, J., Ouyang, H., Jiang, D., Zhao, C., Li, Z., Qu, X., Liu, Z., Fan, Y., Shi, B., et al. (2020). A flexible self-arched biosensor based on combination of piezoelectric and triboelectric effects. Appl. Mater. Today *20*, 100699.

91. Fan, F.-R., Tian, Z.-Q., and Wang, Z.L. (2012). Flexible triboelectric generator. Nano Energy *1*, 328–334.

92. Zheng, Q., Tang, Q., Wang, Z.L., and Li, Z. (2021). Self-powered cardiovascular electronic devices and systems. Nat. Rev. Cardiol. *18*, 7–21.

93. Zou, Y., Bo, L., and Li, Z. (2021). Recent progress in human body energy harvesting for smart bioelectronic system. Fundamental Research. *1*, 364–382.

94. Allataifeh, A., and Al Ahmad, M. (2020). Simultaneous piezoelectric noninvasive detection of multiple vital signs. Sci. Rep. *10*, 416.

95. Zhao, G., Zhang, Y., Shi, N., Liu, Z., Zhang, X., Wu, M., Pan, C., Liu, H., Li, L., and Wang, Z.L. (2019). Transparent and stretchable triboelectric nanogenerator for self-powered tactile sensing. Nano Energy *59*, 302–310.

96. Katsuura, T., Izumi, S., Yoshimoto, M., Kawaguchi, H., Yoshimoto, S., and Sekitani, T. (2017). 2017 IEEE Biomedical Circuits and Systems Conference (BioCAS) (IEEE), pp. 1–4.

97. Niu, Q., Huang, L., Lv, S., Shao, H., Fan, S., and Zhang, Y. (2020). Pulse-driven bio-triboelectric nanogenerator based on silk nanoribbons. Nano Energy *74*, 104837.

98. Wang, R., Mu, L., Bao, Y., Lin, H., Ji, T., Shi, Y., Zhu, J., and Wu, W. (2020). Holistically engineered polymer-polymer and polymer-ion interactions in biocompatible polyvinyl alcohol blends for high-performance triboelectric devices in self-powered wearable cardiovascular monitorings. Adv. Mater. *32*, e2002878.

99. Boutry, C.M., Beker, L., Kaizawa, Y., Vassos, C., Tran, H., Hinckley, A.C., Pfattner, R., Niu, S., Li, J., Claverie, J., et al. (2019). Biodegradable and flexible arterial-pulse sensor for the wireless monitoring of blood flow. Nat. Biomed. Eng. *3*, 47–57.

100. Wang, Z., Cui, H., Li, S., Feng, X., Aghassi-Hagmann, J., Azizian, S., and Levkin, P.A. (2021). Facile approach to conductive polymer microelectrodes for flexible electronics. ACS Appl. Mater. Interfaces *13*, 21661–21668.

101. Sharma, S., Chhetry, A., Sharifuzzaman, M., Yoon, H., and Park, J.Y. (2020). Wearable capacitive pressure sensor based on MXene composite nanofibrous scaffolds for reliable human physiological signal acquisition. ACS Appl. Mater. Interfaces *12*, 22212–22224.

102. Guo, Y., Gao, S., Yue, W., Zhang, C., and Li, Y. (2019). Anodized aluminum oxide-assisted low-cost flexible capacitive pressure sensors based on double-sided nanopillars by a facile fabrication method. ACS Appl. Mater. Interfaces *11*, 48594–48603.

103. Lin, M.-F., Xiong, J., Wang, J., Parida, K., and Lee, P.S. (2018). Core-shell nanofiber mats for tactile pressure sensor and nanogenerator applications. Nano Energy *44*, 248–255.

104. Pang, C., Koo, J.H., Nguyen, A., Caves, J.M., Kim, M.G., Chortos, A., Kim, K., Wang, P.J., Tok, J.B., and Bao, Z. (2015). Highly skin-conformal microhairy sensor for pulse signal amplification. Adv. Mater. *27*, 634–640.

105. Jung, Y., Lee, W., Jung, K., Park, B., Park, J., Ko, J., and Cho, H. (2020). A highly sensitive and flexible capacitive pressure sensor based on a porous three-dimensional PDMS/microsphere composite. Polymers (Basel) *12*, 1412.

106. Nassar, J.M., Mishra, K., Lau, K., Aguirre-Pablo, A.A., and Hussain, M.M. (2017). Recyclable nonfunctionalized paper-based ultralow-cost wearable health monitoring system. Adv. Mater. Technol. *2*, 1600228.

107. Zhao, S., Ran, W., Wang, D., Yin, R., Yan, Y., Jiang, K., Lou, Z., and Shen, G. (2020). 3D dielectric layer enabled highly sensitive capacitive pressure sensors for wearable electronics. ACS Appl. Mater. Interfaces *12*, 32023–32030.

108. Lei, Z., Wang, Q., Sun, S., Zhu, W., and Wu, P. (2017). A bioinspired mineral hydrogel as a self-healable, mechanically adaptable ionic skin for highly sensitive pressure sensing. Adv. Mater. *29*, 1700321.

109. Zhu, Z., Li, R., and Pan, T. (2018). Imperceptible epidermal-iontronic interface for wearable sensing. Adv. Mater. *30*, 1705122.

110. Asada, H.H., and Hutchinson, R.C. (2001). A new ring sensor design for improved motion artifact reduction without circulatory interference (Progress Report), pp. 1–45.

111. Chung, H.U., Kim, B.H., Lee, J.Y., Lee, J., Xie, Z., Ibler, E.M., Lee, K., Banks, A., Jeong, J.Y., Kim, J., et al. (2019). Binodal, wireless epidermal electronic systems with in-sensor analytics for neonatal intensive care. Science *363*, eaau0780.

112. Chung, H.U., Rwei, A.Y., Hourlier-Fargette, A., Xu, S., Lee, K., Dunne, E.C., Xie, Z., Liu, C., Carlini, A., Kim, D.H., et al. (2020). Skin-interfaced biosensors for advanced wireless physiological monitoring in neonatal and pediatric intensive-care units. Nat. Med. *26*, 418–429.

113. Polat, E.O., Mercier, G., Nikitskiy, I., Puma, E., Galan, T., Gupta, S., Montagut, M., Piqueras, J.J., Bouwens, M., Durduran, T., et al. (2019). Flexible graphene photodetectors for wearable fitness monitoring. Sci. Adv. *5*, eaaw7846.

114. Lee, H., Kim, E., Lee, Y., Kim, H., Lee, J., Kim, M., Yoo, H.-J., and Yoo, S. (2018). Toward all-day wearable health monitoring: An ultralow-power, reflective organic pulse oximetry sensing patch. Sci. Adv. *4*, eaas9530.

115. Xu, H., Liu, J., Zhang, J., Zhou, G., Luo, N., and Zhao, N. (2017). Flexible organic/inorganic hybrid near-infrared photoplethysmogram sensor for cardiovascular monitoring. Adv. Mater. *29*, 1700975.

116. Kim, T.H., Lee, C.S., Kim, S., Hur, J., Lee, S., Shin, K.W., Yoon, Y.Z., Choi, M.K., Yang, J., Kim, D.H., et al. (2017). Fully stretchable optoelectronic sensors based on colloidal quantum dots for sensing photoplethysmographic signals. ACS Nano *11*, 5992–6003.

117. Zhang, G., Liu, M., Guo, N., and Zhang, W. (2016). Design of the MEMS piezoresistive electronic heart sound sensor. Sensors (Basel) *16*, 1728.

118. Wang, W., Xu, Q., Zhang, G., Lian, Y., Zhang, L., Zhang, X., Shi, Y., Duan, S., and Wang, R. (2019). A bat-shape piezoresistor electronic stethoscope based on MEMS technology. Measurement *147*, 106850.

119. Pei, Y., Wang, W., Zhang, G., Ding, J., Xu, Q., Zhang, X., Yang, S., Shen, N., Lian, Y., Zhang, L., et al. (2019). Design and implementation of T-type MEMS heart sound sensor. Sens. Actuators A Phys. *285*, 308–318.

120. Cotur, Y., Kasimatis, M., Kaisti, M., Olenik, S., Georgiou, C., and Güder, F. (2020). Stretchable composite acoustic transducer for wearable monitoring of vital signs. Adv. Funct. Mater. *30*, 1910288.

121. Nayeem, M.O.G., Lee, S., Jin, H., Matsuhisa, N., Jinno, H., Miyamoto, A., Yokota, T., and Someya, T. (2020). All-nanofiber-based, ultrasensitive, gas-permeable mechanoacoustic sensors for continuous long-term heart monitoring. Proc. Natl. Acad. Sci. USA *117*, 7063–7070.

122. Kim, J.H., Kim, S.R., Kil, H.J., Kim, Y.C., and Park, J.W. (2018). Highly conformable, transparent electrodes for epidermal electronics. Nano Lett. *18*, 4531–4540.

123. Zhou, W., Yao, S., Wang, H., Du, Q., Ma, Y., and Zhu, Y. (2020). Gas-permeable, ultrathin, stretchable epidermal electronics with porous electrodes. ACS Nano *14*, 5798–5805.

124. Nawrocki, R.A., Jin, H., Lee, S., Yokota, T., Sekino, M., and Someya, T. (2018). Self-adhesive and ultra-conformable, sub-300 nm dry thin-film electrodes for surface monitoring of biopotentials. Adv. Funct. Mater. *28*, 1803279.

125. He, K., Liu, Z., Wan, C., Jiang, Y., Wang, T., Wang, M., Zhang, F., Liu, Y., Pan, L., Xiao, M., et al. (2020). An on-skin electrode with anti-epidermal-surface-lipid function based on a zwitterionic polymer brush. Adv. Mater. *32*, e2001130.

126. Yeo, W.H., Kim, Y.S., Lee, J., Ameen, A., Shi, L., Li, M., Wang, S., Ma, R., Jin, S.H., Kang, Z., et al. (2013). Multifunctional epidermal electronics printed directly onto the skin. Adv. Mater. *25*, 2773–2778.

127. Kabiri Ameri, S., Ho, R., Jang, H., Tao, L., Wang, Y., Wang, L., Schnyer, D.M., Akinwande, D., and Lu, N. (2017). Graphene electronic tattoo sensors. ACS Nano *11*, 7634–7641.

128. Gan, D., Huang, Z., Wang, X., Jiang, L., Wang, C., Zhu, M., Ren, F., Fang, L., Wang, K., Xie, C., and Lu, X. (2019). Graphene oxide-templated conductive and redox-active nanosheets incorporated hydrogels for adhesive bioelectronics. Adv. Funct. Mater. *30*, 1907678.

129. Sun, B., McCay, R.N., Goswami, S., Xu, Y., Zhang, C., Ling, Y., Lin, J., and Yan, Z. (2018). Gas-permeable, multifunctional on-skin electronics based on laser-induced porous graphene and sugar-templated elastomer sponges. Adv. Mater. *30*, e1804327.

130. Chun, S., Kim, D.W., Baik, S., Lee, H.J., Lee, J.H., Bhang, S.H., and Pang, C. (2018). Conductive and stretchable adhesive electronics with miniaturized octopus-like suckers against dry/wet skin for biosignal monitoring. Adv. Funct. Mater. *28*, 1805224.

131. Son, D., Kang, J., Vardoulis, O., Kim, Y., Matsuhisa, N., Oh, J.Y., To, J.W., Mun, J., Katsumata, T., Liu, Y., et al. (2018). An integrated self-healable electronic skin system fabricated via dynamic reconstruction of a nanostructured conducting network. Nat. Nanotechnol. *13*, 1057–1065.

132. Ershad, F., Thukral, A., Yue, J., Comeaux, P., Lu, Y., Shim, H., Sim, K., Kim, N.I., Rao, Z., Guevara, R., et al. (2020). Ultra-conformal drawn-on-skin electronics for multifunctional motion artifact-free sensing and point-of-care treatment. Nat. Commun. *11*, 3823.

133. Fan, Y.J., Yu, P.T., Liang, F., Li, X., Li, H.Y., Liu, L., Cao, J.W., Zhao, X.J., Wang, Z.L., and Zhu, G. (2020). Highly conductive, stretchable, and breathable epidermal electrode based on hierarchically interactive nano-network. Nanoscale *12*, 16053–16062.

134. Xu, S., Zhang, Y., Jia, L., Mathewson, K.E., Jang, K.I., Kim, J., Fu, H., Huang, X., Chava, P., Wang, R., et al. (2014). Soft microfluidic assemblies of sensors, circuits, and radios for the skin. Science *344*, 70–74.

135. Inan, O.T., Migeotte, P.F., Park, K.S., Etemadi, M., Tavakolian, K., Casanella, R., Zanetti, J., Tank, J., Funtova, I., Prisk, G.K., and Di Rienzo, M. (2015). Ballistocardiography and seismocardiography: a review of recent advances. IEEE J. Biomed. Health Inform. *19*, 1414–1427.

136. Inan, O.T., Baran Pouyan, M., Javaid, A.Q., Dowling, S., Etemadi, M., Dorier, A., Heller, J.A., Bicen, A.O., Roy, S., De Marco, T., and Klein, L. (2018). Novel wearable seismocardiography and machine learning algorithms can assess clinical status of heart failure patients. Circ. Heart Fail. *11*, e004313.

137. Etemadi, M., Inan, O.T., Heller, J.A., Hersek, S., Klein, L., and Roy, S. (2016). A wearable patch to enable long-term monitoring of environmental, activity and hemodynamics variables. IEEE Trans. Biomed. Circuits Syst. *10*, 280–288.

138. Liu, Y., Norton, J.J., Qazi, R., Zou, Z., Ammann, K.R., Liu, H., Yan, L., Tran, P.L., Jang, K.-I., Lee, J.W., et al. (2016). Epidermal mechano-acoustic sensing electronics for cardiovascular diagnostics and human-machine interfaces. Sci. Adv. *2*, e1601185.

139. Gupta, P., Moghimi, M.J., Jeong, Y., Gupta, D., Inan, O.T., and Ayazi, F. (2020). Precision wearable accelerometer contact microphones for longitudinal monitoring of mechano-acoustic cardiopulmonary signals. NPJ Digit. Med. *3*, 19.

140. Ha, T., Tran, J., Liu, S., Jang, H., Jeong, H., Mitbander, R., Huh, H., Qiu, Y., Duong, J., Wang, R.L., et al. (2019). A chest-laminated ultrathin and stretchable e-tattoo for the measurement of electrocardiogram, seismocardiogram, and cardiac time intervals. Adv. Sci. (Weinh.) *6*, 1900290.

141. You, I., Kim, B., Park, J., Koh, K., Shin, S., Jung, S., and Jeong, U. (2016). Stretchable E-skin apexcardiogram sensor. Adv. Mater. *28*, 6359–6364.

142. Wang, S., Xu, J., Wang, W., Wang, G.N., Rastak, R., Molina-Lopez, F., Chung, J.W., Niu, S., Feig, V.R., Lopez, J., et al. (2018). Skin electronics from scalable fabrication of an intrinsically stretchable transistor array. Nature *555*, 83–88.

143. Gao, L., Zhang, Y., Malyarchuk, V., Jia, L., Jang, K.-I., Webb, R.C., Fu, H., Shi, Y., Zhou, G., Shi, L., et al. (2014). Epidermal photonic devices for quantitative imaging of temperature and thermal transport characteristics of the skin. Nat. Commun. *5*, 4938.

144. Webb, R.C., Ma, Y., Krishnan, S., Li, Y., Yoon, S., Guo, X., Feng, X., Shi, Y., Seidel, M., Cho, N.H., et al. (2015). Epidermal devices for noninvasive, precise, and continuous mapping of macrovascular and microvascular blood flow. Sci. Adv. *1*, e1500701.

145. Fu, Y., Zhao, S., Wang, L., and Zhu, R. (2019). A wearable sensor using structured silver-particle reinforced PDMS for radial arterial pulse wave monitoring. Adv. Healthc. Mater. *8*, e1900633.

146. Wang, J., Liu, K., Sun, Q., Ni, X., Ai, F., Wang, S., Yan, Z., and Liu, D. (2019). Diaphragm-based optical fiber sensor for pulse wave monitoring and cardiovascular diseases diagnosis. J. Biophotonics *12*, e201900084.

147. Leitão, C., Antunes, P., Pinto, J., Mesquita Bastos, J., and André, P. (2016). Optical fiber sensors for central arterial pressure monitoring. Opt. Quantum Electron. *48*, 218.